Available online at www.sciencedirect.com
ScienceDirect
Marine Micropaleontology 62 (2007) 211–234
MARINE MICROPALEONTOLOGY
www.elsevier.com/locate/marmicro

Danian/Selandian boundary stratigraphy, paleoenvironment and Ostracoda from Sidi Nasseur, Tunisia

Jimmy Van Itterbeeck [a,*], Jorinde Sprong [a], Christian Dupuis [b], Robert P. Speijer [a], Etienne Steurbaut [a,c]

[a] *Department of Geography and Geology, KULeuven, Celestijnenlaan 200E, 3001 Leuven, Belgium*
[b] *GFA, Faculté Polytechnique de Mons, 9 Rue de Houdain, 9000 Mons, Belgium*
[c] *Royal Belgian Institute of Natural Sciences, Vautierstraat 29, 1000 Brussel, Belgium*

Received 30 January 2006; received in revised form 26 July 2006; accepted 8 August 2006

Abstract

Two detailed records (NSF and 05NSC, Sidi Nasseur, Tunisia) across the Danian/Selandian (D/S) boundary were investigated for their micropaleontological content. Calcareous nannofossils and planktic foraminifera provided a biostratigraphic framework. The interval spans part of planktic foraminiferal Zone P2, Subzone P3a and part of Subzone P3b. This corresponds to calcareous nannoplankton Zone NP4. Using a more detailed nannofossil zonation the studied section spans part of Zone NTp6, Zone NTp7a and part of NTp7b. Quantitative ostracod and qualitative benthic foraminiferal data were used to characterize environmental changes across the D/S boundary. The two subsections have yielded a total of 50 ostracod taxa. The ostracod assemblage of the entire section belongs to the Southern Tethyan Type showing subtle but distinct changes up section. Based on statistical analysis of the quantitative ostracod data, faunal changes at a glauconitic maker bed (P3a/P3b boundary) were demonstrated. The local *Reticulina proteros* assemblage, with the typical species *R. proteros*, *Oertliella vesiculosa* and *Cytheroptheron lekefense,* is gradually replaced by the *Protobuntonia nakkadii* assemblage, with the typical species *Cristaeleberis arabii*, *Xestoleberis tunisiensis*, *Cytheropteron* sp. and *P. nakkadii*, across the glauconitic bed. The benthic foraminifera also demonstrated distinct changes at this marker bed. The changes in ostracods and foraminifera are related to changes in paleoproductivity and an overall relative sea-level fall.

The lithological and faunal changes at the P3a/P3b zone boundary within the Sidi Nasseur sections seem to correspond to the D/S boundary in the type region in Danmark and are characterized by a significant hiatus, yielding this section not suitable as a GSSP candidate for this boundary.

Keywords: Danian/Selandian boundary; Tunisia; Tethys; Ostracoda; Benthic foraminifera

1. Introduction

Since its definition by Schimper (1874), the Paleocene Series has been a subject of discussion. For a long time, it met with opposition before being internationally accepted as the lowermost series of the Paleogene. Its subdivision has also been the subject of much controversy (Gradstein et al., 2004, fig. 1.7b for an overview).

* Corresponding author. Current affiliation: Exploration geologist, Shell International Exploration and Production, Kesslerpark 1, 2288GS Rijswijk, The Netherlands. Tel.: +31 704473722.
E-mail addresses: jvanitterbeeck@yahoo.co.uk (J. Van Itterbeeck), jorinde.sprong@geo.kuleuven.be (J. Sprong), christian.dupuis@fpms.ac.be (C. Dupuis), robert.speijer@geo.kuleuven.be (R.P. Speijer), etienne.steurbaut@naturalsciences.be (E. Steurbaut).

0377-8398/$ - see front matter © 2006 Elsevier B.V. All rights reserved.
doi:10.1016/j.marmicro.2006.08.006

In the past, several authors favored a twofold subdivision of the Paleocene. But even among them there was disagreement on the appropriate stage spanning the upper Paleocene as both Thanetian and Selandian were used. Recently, a threefold subdivision into the Danian, Selandian and Thanetian Stages has been approved (Berggren et al., 1995). Most research efforts on the Paleocene Series have been invested in both its lower and upper boundaries: the Cretaceous/Paleogene (K/P) and Paleocene/Eocene (P/E) boundary, respectively. As both boundaries are characterized by drastic faunal, floral and environmental change, they have drawn the attention of many scientists around the globe. Compared to its boundaries, the remainder of the Paleocene has received little attention. As a consequence, the stratigraphy of the Paleocene still contains a number of unresolved problems. Two of those, the age and characteristics of the Danian/Selandian (D/S) boundary are the subject of the present study.

The Danian Stage was introduced by Desor (1847) and is named after its type area in Denmark. It comprises the Paleocene chalks and limestones overlying the Maastrichtian chalks. Because of the lithological similarities between the Danian and Maastrichtian in NW Europe, the Danian was long considered the upper stage of the Cretaceous. The Selandian Stage is composed of greensands, marls and clays overlying Danian limestones in Denmark (Rosenkrantz, 1924). The stage was named after the Danish island of Zealand. Like most of the Paleogene stages, both the Danian and Selandian have been defined in the North Sea Basin. However, these sequences are difficult to correlate on a global scale. The D/S boundary in Danish outcrop sections is characterized by a hiatus. Only recently, the duration of this hiatus has been precisely estimated in the different sections in the type region (Clemmensen and Thomsen, 2005). In addition, there is no agreement on a guide event for this boundary. Berggren et al. (1995, 2000) favored the delineation of the D/S boundary by the planktic foraminiferal P2/P3a subzonal boundary, defined by the lowest occurrence of the *Praemurica uncinata* and with an estimated age of 60.9 Ma. Alternatively, Schmitz et al. (1998) proposed to correlate it with a level close to the base of calcareous nannofossil Zone NP5, defined by the lowest occurrence of *Fasciculithus tympaniformis*, which is well above the P2/P3a subzonal boundary (Berggren et al., 1995, 2000). Hardenbol et al. (1998) correlated the sequence boundary (Sel1) between the Danian and Selandian with a level within Zone P3a at 60.7 Ma. Consequently a clear stratigraphic framework and nomenclature for this interval are still lacking and there is no approved global boundary stratotype section and point (GSSP) available. However, two candidates have been proposed: the Zumaya section in Northern Spain (Schmitz et al., 1998) and the Sidi Nasseur section in Tunisia (Steurbaut et al., 2000), studied in the present paper. Other potential candidates are situated in Egypt (Speijer, 2003; Guasti, 2005) but have not been proposed as such.

The data presented here summarize the current state of knowledge on the Sidi Nasseur section (Steurbaut et al., 2000), with special emphasis on the ostracod data. Rich ostracod assemblages have been described from the Campanian–Eocene interval of the nearby El Kef (Esker, 1968; Donze et al., 1982) and Elles (Said, 1978) sections, but these have not been studied quantitatively. The present paper provides the first quantitative record on Paleocene ostracods from Tunisia and as such it aims at shedding new light on biotic and paleoenvironmental changes associated with the D/S transition in this region.

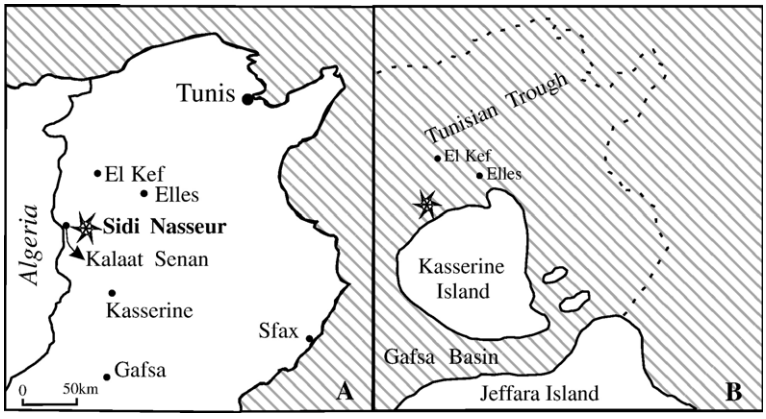

Fig. 1. A. Location of the Sidi Nasseur sections within Tunisia (white areas are emerged); B. Paleogeographic situation of northern Tunisia during the Paleocene (modified after Zaier et al., 1998).

2. Geological setting

The Sidi Nasseur section is situated near the village of Kalaat Senan in central Tunisia near the Algerian border (Fig. 1A). From a paleogeographic point of view, the section is situated in the southern Tethys in the proximal part of the Tunisian Trough near the emerged Kasserine Island (Fig. 1B). During the late Mesozoic and the early Cenozoic shallow seas covered most of Tunisia. By the end of the Cretaceous, the Jeffara and Kasserine Islands and other small areas emerged in south and central Tunisia (Zaier et al., 1998). Paleocene sediments in the Tunisian Trough (= Sillon Tunésien or northern basins) are up to 500 m thick due to a high subsidence rate and sediment input, but their thickness reduces towards the Kasserine Island. During most of the early and early late Paleocene, the Sidi Nasseur area was characterized by a fairly uniform, marly hemipelagic sedimentation regime. The marls, informally known as the Aïn Settara Marls (Steurbaut et al., 2000), belong to the El Haria Formation (Burollet, 1956, p.132–138). The El Haria Formation ranges from Maastrichtian to Ypresian and at El Kef the GSSP for the base of the Danian Stage (= K/P boundary) was defined within this formation (Cowie et al., 1989; Remane et al., 1999). It overlies the Campanian–Maastrichtian chalky limestones of the Abiod Formation and it is overlain by limestones and phosphates of the Ypresian Metlaoui Formation (see Dupuis et al., 2001, fig. 1 for a lithostratigraphic column of the area).

3. Material and methods

We investigated two subsections below the hill top of Sidi Nasseur: NSF, the Sidi Nasseur section of Steurbaut et al. (2000) and 05NSC, a partial lateral equivalent, only 50 m south of NSF. NSF comprises a 17 m thick interval spanning the D/S transition in which 42 samples were taken. 05NSC comprises an 8 m thick interval spanning the D/S transition in which 21 samples were taken. Guasti et al. (2006) discussed the stratigraphy and paleoenvironmental setting of the Aïn Settara (ASP) section, which is another lateral equivalent about 1 km south of the NSF/05NSC sections.

The most striking feature of the Sidi Nasseur sections is a 50–80 cm thick glauconitic marker bed topping a complex channel system that complicates the correlation between both sections. For correlation between the subsections, the glauconitic marker bed and biostratigraphic boundaries (Fig. 2) were used. Based on the proposed correlation, corresponding levels of the 05NSC-samples were projected onto the NSF-section. This combined succession was used to plot the results from our analysis.

All samples were processed for calcareous nannofossils. Smear-slides were made using standard procedures and examined with a light microsope at 1000× or 1250× magnification.

For ostracod and foraminiferal studies, 21 samples of the NSF section and 7 samples of the 05NSC section were investigated (about one sample per meter). All samples were dried during at least 24 h in a stove at 60 °C. The dry samples were weighed and subsequently soaked in a 50 g/l soda (Na_2CO_3) solution. After at least 1 day, the samples were washed over 2 mm and 63 μm sieves. The residues were dried and the procedure repeated one more time. Usually, this was sufficient to remove all clay and silt. If the sample was still dirty after two runs, it was treated with the tenside Rewoquat®. The clean residue was dried and split into five fractions: >630 μm, >250 μm, >180 μm, >125 μm and >63 μm. More than 300 ostracods from the three fractions >180 μm were picked. Where ostracods were too abundant to pick all specimens, samples were split with a microsplitter and counts were recalculated to the total abundance. The number of individuals of each species is the sum of the adult carapaces and the largest number of either right or left adult valves. The smaller fractions (<180 μm) only contained scarce juvenile ostracods. Counts were made of the total number of picked ostracods and of the fraction >250 μm. A correspondence analysis was run on both datasets using PAST-software (Hammer et al., 2001).

Benthic foraminifera were picked from a split of the 125–630 μm fraction. Representative aliquots, containing 200–300 benthic foraminiferal specimens, were split using an Otto microsplitter. The picked specimens were glued on permanent slides, identified and counted. Dry weighing prior to processing the samples enabled the calculation of numbers of planktic and benthic foraminifera per gram of dry sediment. Qualitative distributions of benthic and planktic foraminifera have been determined enabling the calculation of percentages of planktonic foramininfera in the total foraminiferal fauna (*P*/*B* ratio). Counting was performed on random squares of a picking tray, until 100 specimens of one of the groups was encountered; The *P*/*B* ratio was expressed as $100 * P/(P+B)$. Selected planktic foraminifera were picked (Plate I) and together with calcareous nannofossil data a biostratigraphic framework was constructed.

4. Calcareous nannoplankton

The Sidi Nasseur section spans calcareous nannofossil Zones–Subzones NTp6, NTp7A and NTp7B, corresponding to the middle part of Zone NP4 (Martini,

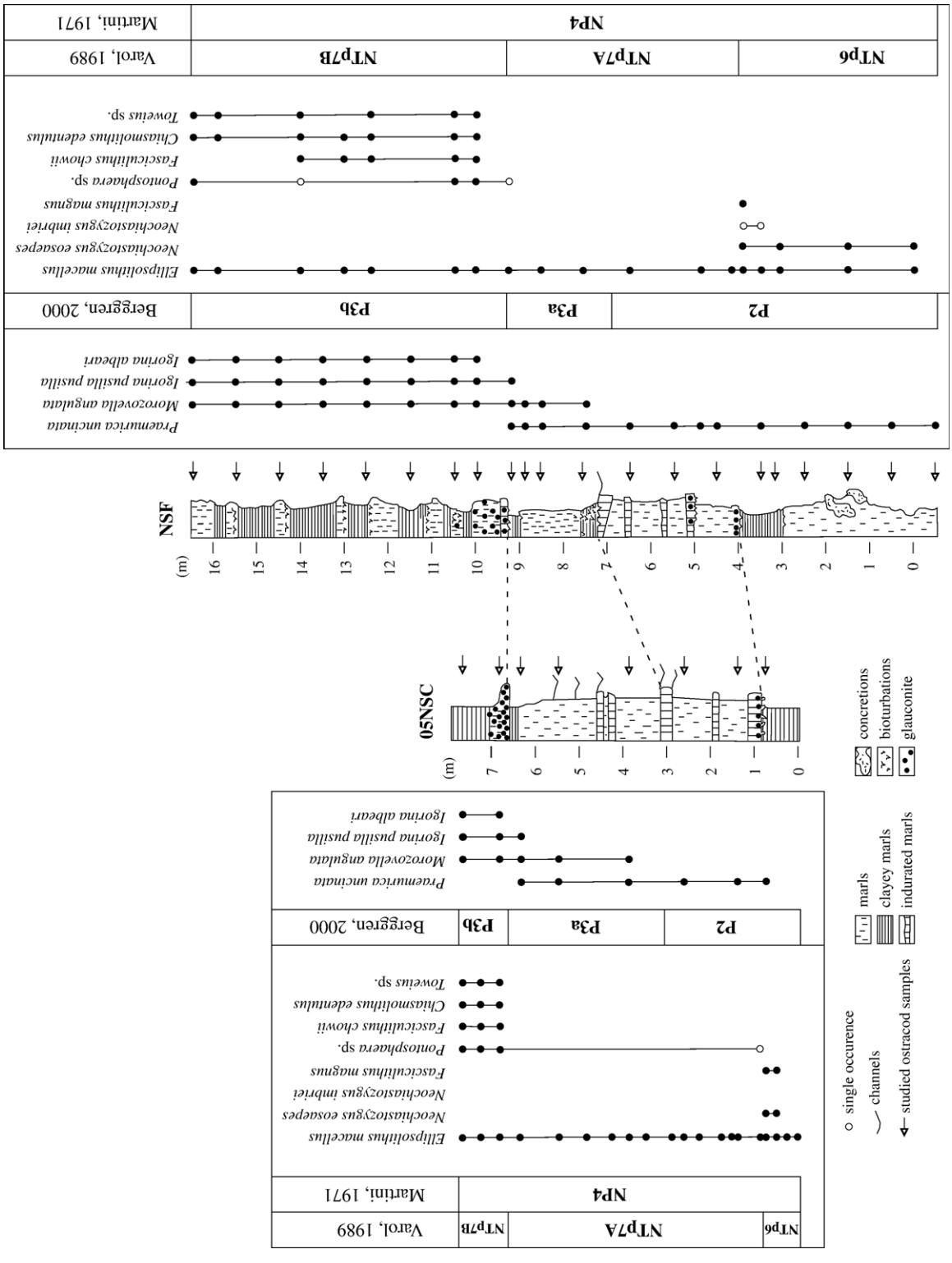

Fig. 2. Litho- and biostratigraphy of the Danian/Selandian boundary interval of the Sidi Nasseur sections.

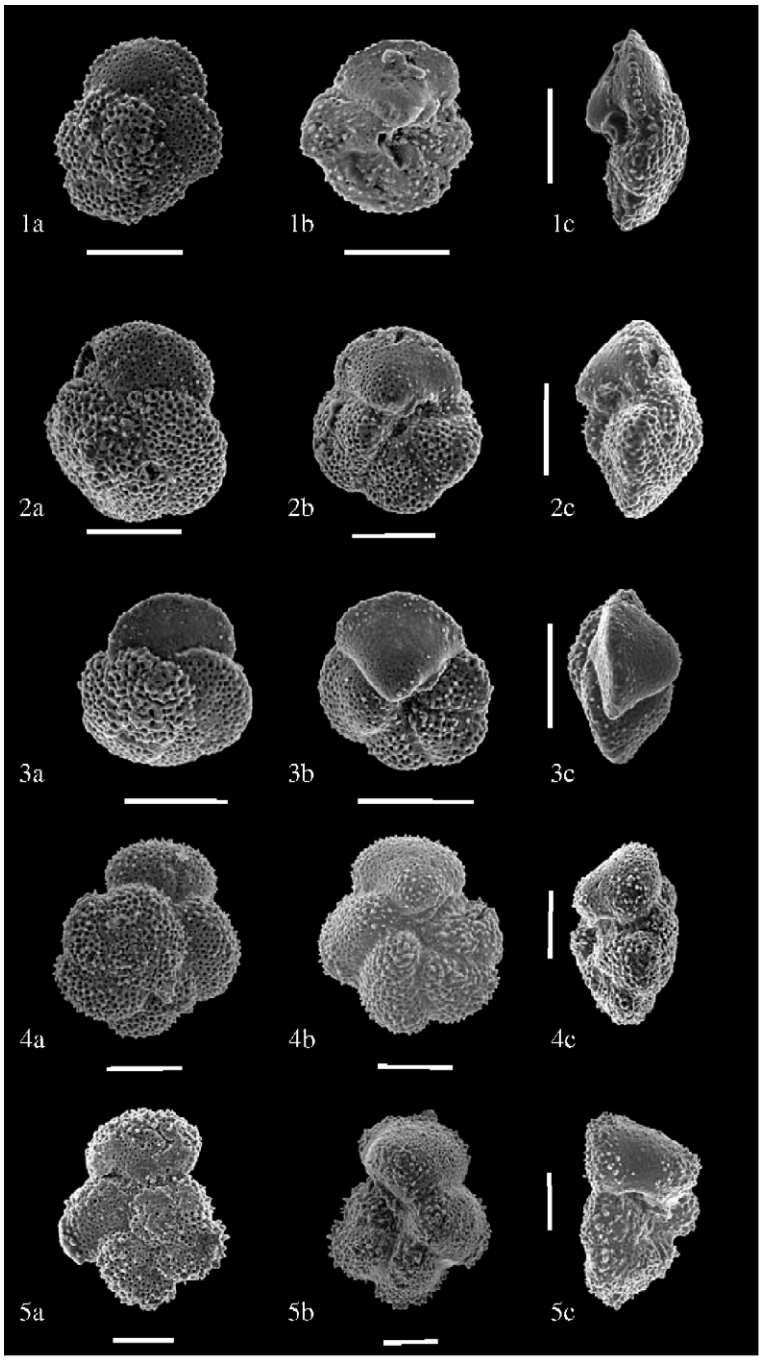

Plate I. Planktic foraminiferal zonal markers: 1–3, *Igorina albeari*: 1, sample NSF10.0 m; 2, sample 05NSC21 (7.6 m); 3, typical *I. albeari* from sample NSF16.5 m. 4, *Morozovella* sp, sample NSF8.0 m. 5, *Morozovella angulata*, sample NSF8.0 m. a = spiral view, b = umbilical view, c = apertural view, scale bar = 100 μm.

1971; Varol, 1989). The highest occurrence (HO) of *Neochiastozygus imbriei* and *N. eosaepes*, defining the NTp6/NTp7A subzonal boundary, have been identified in samples NSF 3.90 m and 05NSC 3, the lowest occurrence (LO) of *Chiasmolithus edentulus*, marking the NTp7A/NTp7B subzonal boundary, in samples NSF 10,0 m and 05NSC 19. As *Sphenolithus primus* was not encountered in the sample sets, it is assumed that the top of the NSF section is still within Subzone NTp7B. These data are in full agreement with the results of earlier nannofossil

studies and interpretations of the NSF section (Steurbaut et al., 2000) and the partly equivalent ASP section discussed by Guasti et al. (2006). It demonstrates that at low latitudes the first consistent occurrence of the genus *Fasciculithus* is a distinct event within Zone NP4 and that it coincides with the LO of *C. edentulus*. The detailed sampling of the 05NSC section (every 25 cm) reveals for the first time that in Tunisia this *Fasciculithus* event is preceded by an ephemeral occurrence of *Fasciculithus magnus* (very low numbers in a ~ 40 cm interval: only in 05NSC 2 and 3 and in NSF 3.90 m, a sample not studied earlier). This short-ranged occurrence, which can easily be overlooked, is located at the top of Subzone NTp6. The observations indicate that at Sidi Nasseur Subzone NTp7A is a *Fasciculithus*-free interval.

The general composition of the associations does not fundamentally vary through the section (about 85% of the taxa are ubiquitous). Despite this marked uniformity, substantial biotic change has been recorded at two specific levels: the top of the lowermost clay unit and the base of the upper thick glauconitic bed, about 5 m up section (at 4 m and at 9.30 m in NSF and at 0.85 m and 6.63 m in 05NSC, respectively). The lower event is marked by a series of HOs (*F. magnus*, *N. imbriei* and *N. eosaepes*), denoting the NTp6–NTp7A subzonal boundary (see above), the upper event by a major increase in species diversity, among which are the LOs of *C. edentulus*, *Fasciculithus chowii* and another unnamed *Fasciculithus*, the LO of *Toweius* sp. (middle-sized elliptical form) and the start of the consistent occurrence (several specimens in each sample) of *Pontosphaera* sp. Both events coincide with omission surfaces at the base of glauconite levels, indicating hiati, or at least condensation.

5. Planktic foraminifera

The studied part of the Sidi Nasseur section starts in Zone P2, defined as the interval between the LO of *P. uncinata* and the LO of *Morozovella angulata* (Berggren et al., 1995). Zone P3 is defined as the stratigraphic interval between the LO of *M. angulata* and the LO of *Globanomalina pseudomenardii*. Zone P3 is divided into Subzones P3a and P3b based on the LO of *Igorina albeari* at the base of zone P3b. Both the P2/P3a and P3a/b zonal boundaries have been identified in the NSF and 05NSC subsections. The P2/P3a zonal boundary has been recognized at the base of a yellow-colored channel bed and the P3a/b zonal boundary coincides with the base of the glauconitic marker bed. Subzone P3a spans only 2 m at NSF and 3 m at 05NSC. Subzone P3b is more expanded and continues above the studied interval. The planktic foraminiferal biostratigraphy proposed in this study for the Sidi Nasseur sections differs from that proposed for the NSF section by Steurbaut et al. (2000, fig. 2). In that study, *M. angulata* was not found below the glauconitic marker bed. However, we observed distinctly keeled specimens of *M. angulata*, within the short interval below the glauconitic bed (Plate I). In addition, we observed slightly keeled specimens of *I. albeari* from the glauconitic bed upwards marking the base of Subzone P3b. This again contrasts with the earlier observations of Molina (in Steurbaut et al., 2000) who found the LO of this species much higher up section. Our planktic foraminiferal results are in agreement with those of Guasti et al. (2006) on the nearby Aïn Settara ASP section.

The channel-like surface at the P2/3 zonal boundary marks a hiatus of uncertain duration. This duration is considered to be quite limited considering the short duration of Biochron P2 (0.2 m.y.; Berggren et al., 1995) and the large thickness (>7 m) of Zone P2 in the section. The P3a/P3b transition is also marked by a hiatus in the Sidi Nasseur sections. Considering the duration of Subbiochron P3a (~ 1 m.y.) and its very limited stratigraphic thickness within the Sidi Nasseur sections, a considerable amount of Zone P3a seems to be missing.

6. Benthic foraminifera

Two main benthic foraminiferal assemblages can be observed in the studied interval at Sidi Nasseur. The transition between both assemblages coincides with the unconformity at the glauconitic marker bed. The lower *Pulsiphonina prima* assemblage is characterized by frequent occurrences of *P. prima*, *Anomalinoides susanaensis*, *Cibicidoides pseudoacutus* and *Spiroplectinella dentata* besides many other neritic taxa. The important changes in benthic foraminiferal faunas occur around the truncated zonal boundaries. The characteristic deep outer neritic species *Angulogavelinella avnimelechi* disappears just beneath the P2/P3 zonal boundary (Fig. 3). *Anomalinoides affinis* and *Angulogavelinella abudurbensis* gradually decrease in numbers until they disappear at the P3a/P3b Subzonal boundary at the base of the glauconitic marker bed. The upper "Buliminid" assemblage is characterized by a larger number of triserial species that occur frequently above the glauconitic marker bed (Fig. 3). The buliminids make up ~ 50% of the total assemblage in the upper part of the section, which contrasts to the lower part, where they constitute <20% of the total assemblage. Typical taxa of this "Buliminid" assemblage are *Bulimina midwayensis*, *Bulimina strobila*, *Stainforthia* sp., *Uvigerinella* sp. and *Stilostomella*

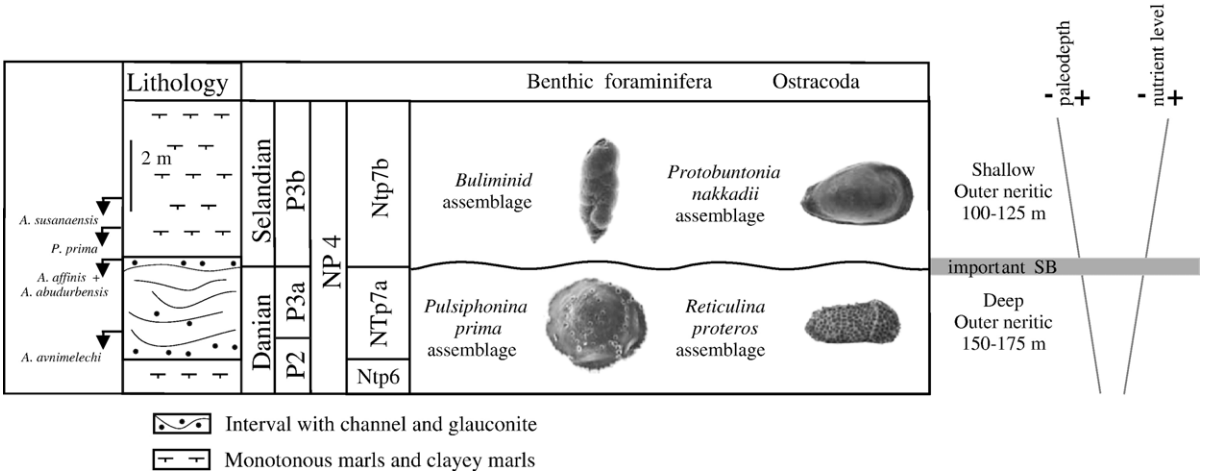

Fig. 3. Sedimentological characteristics and faunal succession of the Danian/Selandian transition in the Sidi Nasseur sections, Tunisia (the trends of paleodepth and nutrient levels are indicated schematically).

plummerae. *A. susanaensis* and *P. prima* have their HOs just above the P3a/b subzonal boundary.

Several foraminiferal parameters have been determined throughout the section (Fig. 4) as they can be indicative of taphonomic features such as dissolution. A combination of high percentages of non-calcareous arenaceous benthic foraminifera, low amounts of planktic and benthic foraminifera per gram of sediment, and low planktic/benthic (*P*/*B*) ratios (expressed as the percentage of planktic specimens in the total number of foraminifera) can be good indications for dissolution (e.g. Speijer and Schmitz, 1998). When combining these data with the calcite content (Steurbaut et al., 2000, fig. c2) and ostracod quantities, several beds that were prone to a considerable degree of dissolution have been identified (Fig. 4): the clayey marl in the lower part of the section (3.5 m), the clayey marl just below the glauconitic marker bed (9.2 m), and the clayey marl near the top of the NSF section (13.6 m).

The top of the main glauconite at 10 m has the lowest percentages of non-calcareous taxa (~ 1%), together with highest amounts of benthic and planktic foraminifera (4600 and 8600 individuals/g, respectively). These data are indicative of condensation and/or winnowing of the clay fraction.

6.1. Paleoenvironment

The successive HOs of deeper dwelling benthic foraminifera (Saint-Marc and Berggren, 1988; Speijer and Schmitz, 1998) such as *A. avnimelechi*, *A. abudurbensis*, *A. affinis*, *A. susanaensis*, *S. dentata* and *P. prima* (Fig. 3) through the sections indicate a general shallowing trend. This corresponds to the general shallowing trend during the Paleocene in the Tunisian Trough (Aubert and Berggren, 1976; Salaj, 1980; Donze et al., 1982; Kouwenhoven et al., 1997). The transition of benthic foraminiferal assemblages at the main glauconite (= P3a/b subzonal boundary) and the general decrease of *P*/*B* ratios indicates an overall decrease in paleodepth from deep outer neritic (~ 175 m) to shallow outer neritic (~ 125 m) deposition. The slight increase in near-shore dinoflagellate cysts (*Pontosphaera* and *Micrantolithus*) in the glauconite bed in the ASP section also points to a regression related to relative sea-level fall (Guasti et al., 2006). A similar depth decrease at this level has been observed in the El Kef section (Guasti et al., 2005a).

The switch to an assemblage with more buliminid type species at the glauconitic marker bed also indicates a transition to more eutrophic conditions (Jorissen et al., 1995). The P3a/b subzonal boundary thus marks the change from relatively oligotrophic, deep outer neritic waters to more eutrophic, shallow outer neritic conditions, in accordance with the interpretation of Guasti et al. (2006) for the parallel Aïn Settara section.

7. Ostracoda

The ostracod fauna in the Sidi Nasseur sections consists of 50 taxa (Plates II and III) (for a complete taxonomic list see Appendix A); most of them have been previously described from Paleocene deposits in northern Africa. Thirteen taxa were only observed in the NSF section: *Cytherelloidea ainshamsina*, *Bairdia* sp., *Bythocypris eskeri*, *Macrocypris* sp. *Paracypris nigeriensis*, *P.*

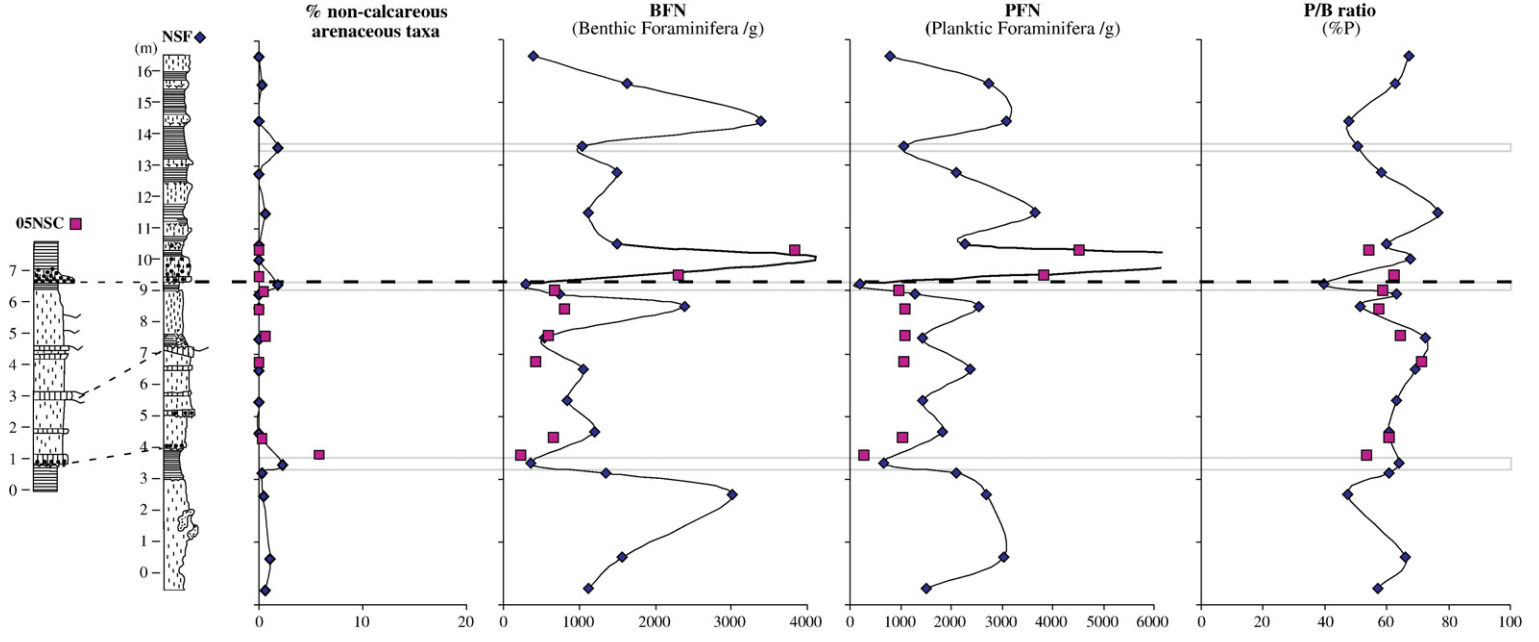

Fig. 4. Foraminiferal parameters plotted against depth of the Sidi Nasseur sections. Grey areas indicate zones of dissolution.

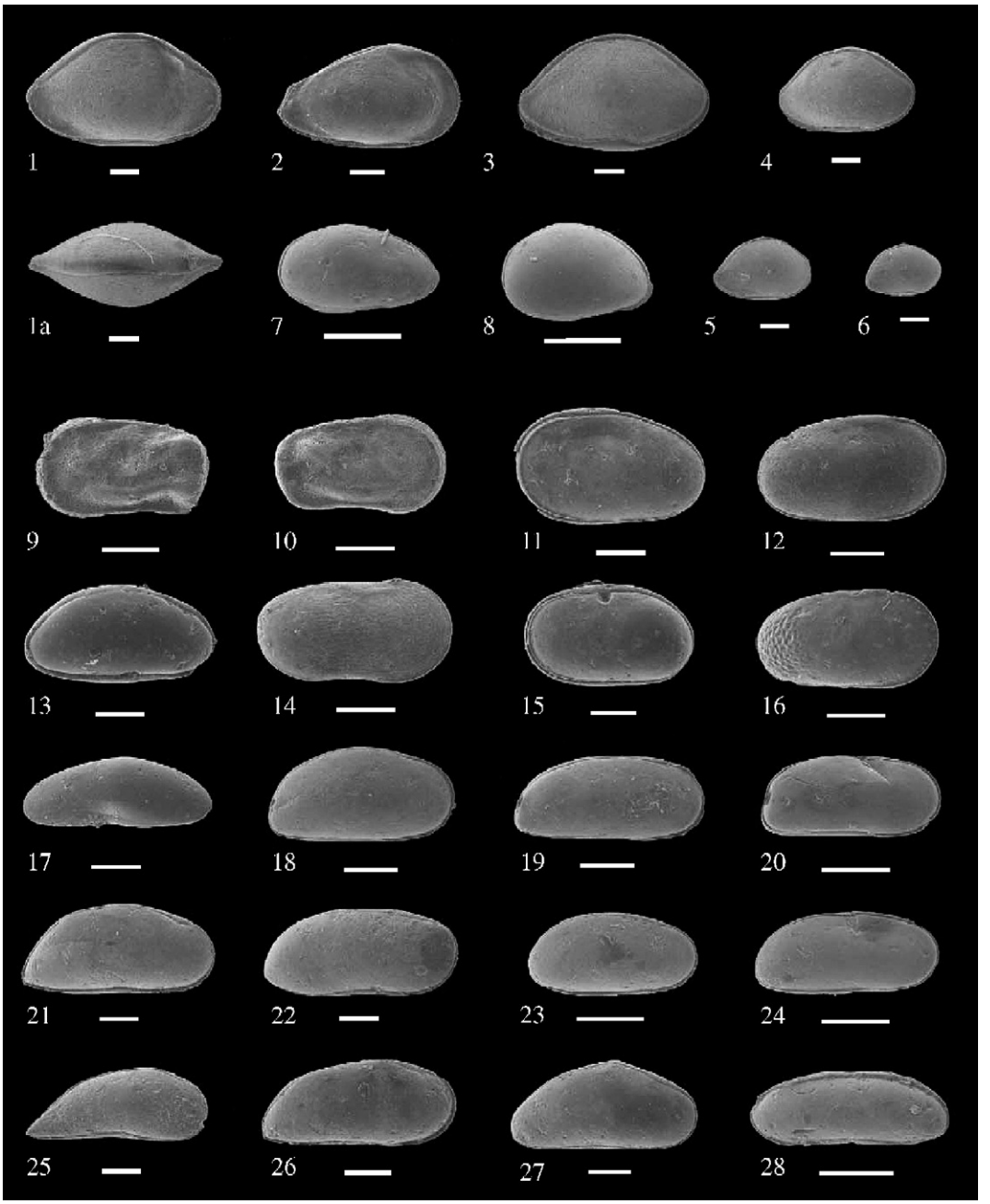

Plate II. 1, *Bairdia malzi* Morsi and Speijer (2003), carapace, adult: a, right view; b, dorsal view. 2, *Protobuntonia nakkadii* Bassiouni (1970), carapace, right view, NSF 15.6 m. 3–6, *Bairdia septentrionalis* Bonnema 1940, carapace, right view, NSF −0.5 m: 3, adult; 4–6, juveniles. 7, *Xestoleberis ovata* Bonnema 1941, carapace, adult, right view, NSF 15.6 m. 8, *Xestoleberis tunisiensis* Esker (1968), carapace, adult, right view, NSF NSF 15.6 m. 9–10, *Cytherelloidea* aff. *melleguensis* Damotte and Said 1984: 9, left valve, female, NSF 15.6 m; 10, right valve, male, NSF 1.5 m. 11–12, *Cytherella sinaensis* Morsi (1999), carapace: 11, left view, female, NSF 3.2 m; 12, right view, male, NSF −0.5 m. 13, *Bythocypris adunca* Esker (1968), carapace, right view, male, NSF-0.5 m. 14, *Cytherella ainshamsina* Bassiouni and Morsi (2000), carapace, right view, NSF 16.5 m. 15, *Cytherella* aff. *lagenalis* Marlière 1958, carapace, left view, NSF 3.2 m. 16, *Cytherella meijeri* Esker (1968), carapace, right view, NSF 15.6 m. 17, *Bythocypris eskeri* Bassiouni and Luger (1990), carapace, left view, NSF −0.5 m. 18–19, *Krithe echolsae* Esker (1968), carapace, right view, NSF −0.5 m: 18, female; 19, male. 20, *Krithe* cf. *solomoni* Honigstein (1984), carapace, right view, NSF 13.6 m. 21, *Paracypris eskeri* Bassiouni and Morsi (2000), carapace, right view, NSF −0.5 m. 22, *Pontocyprella recurva* Esker (1968), carapace, right view, NSF 2.5 m. 23–24, *Parakrithe crolifa* Bassiouni and Luger (1990), carapace, right view, NSF 15.6 m: 23, female; 24, male. 25, *Paracypris jonesi* Bonnema 1941, carapace, right view, NSF 2.5 m. 26, *Paracypris* sp. B Esker (1968), carapace, right view, NSF 1.5 m. 27, *Pontocypris* sp., carapace, right view, NSF 2.5 m. 28, species C, carapace, right view, NSF 5.5 m.

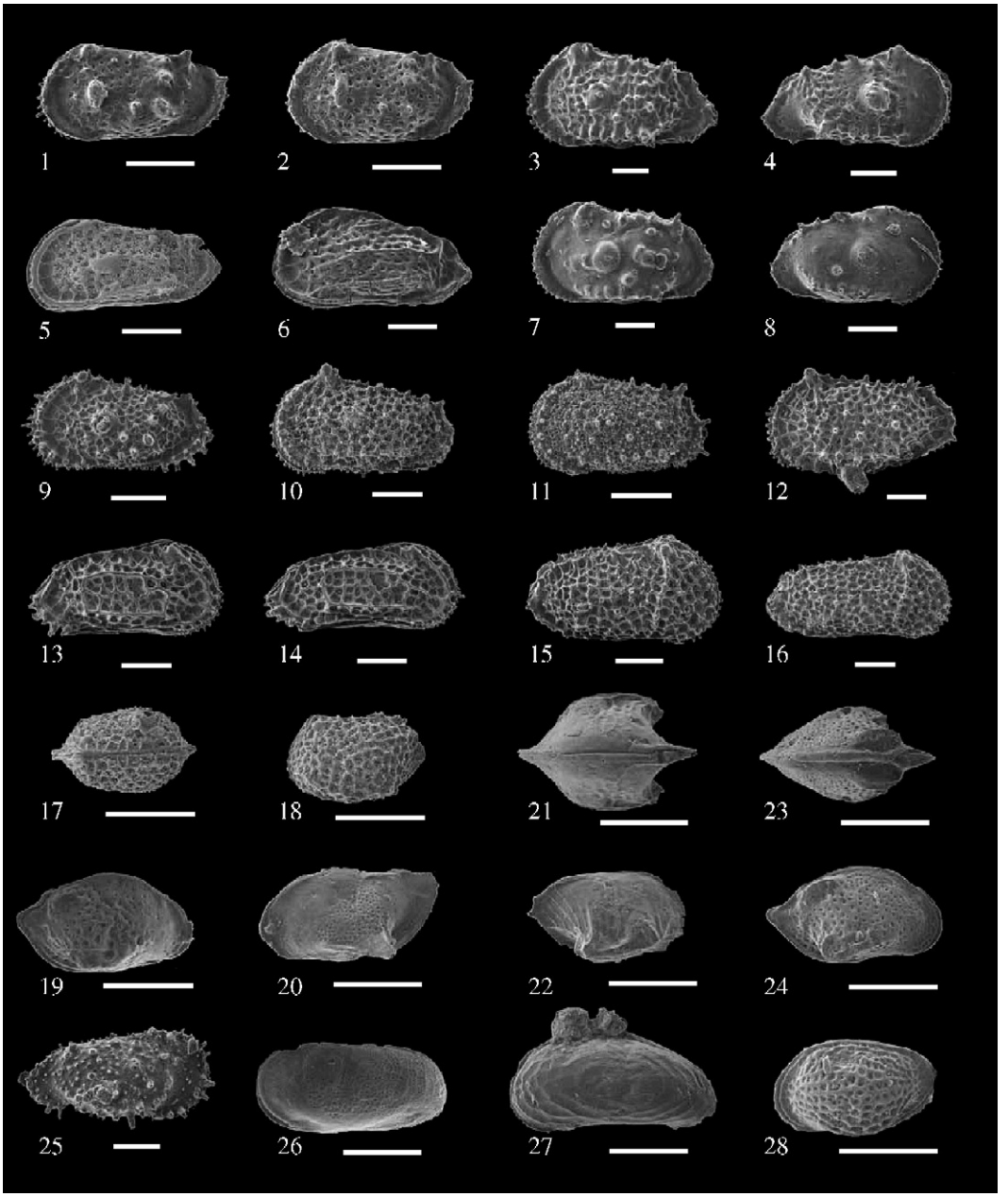

Plate III. 1–2, *Cristaeleberis arabii* Bassiouni (1970), left valve, NSF 12.75 m: 1, morphotype A; 2, morphotype B with pronounced reticulation. 3–4, *Mauritsina jordanica nodosoreticulata* Bassiouni (1970): 3, left valve, adult, NSF −0.5 m; 4, right valve, juvenile, NSF 15.6 m. 5, *Ordoniya ordoniya* (Bassiouni, 1970), carapace, left view, NSF 14.4 m. 6, *Ordoniya bulaqensis* Bassiouni and Luger (1990), carapace, left view, NSF 2.5 m. 7–8, *Mauritsina coronata* (Esker, 1968): 7, left valve, adult, NSF −0.5 m; 8, right valve, juvenile, NSF 2.5 m. 9, *Oertliella posterotriangulata* Morsi (1999), carapace, left view, NSF 14.6 m. 10, *Oertliella delicata* Bassiouni and Luger (1990), carapace, left view, NSF 10.5 m. 11, *Oertliella vesiculosa* (Apostolescu 1961), carapace, left view, NSF 2.5 m. 12, *Megommatocythere denticulata* (Esker, 1968), left valve, external view, NSF 2.5 m. 13–14, *Paracosta parakefensis* Bassiouni and Luger (1990), carapace, right view, NSF 14.4 m: 13, female; 14, male. 15–16: *Reticulina proteros* (Bassiouni, 1969), carapace, right view, NSF −0.5 m: 15, female; 16, male. 17–18, *Eucytherura* aff. *hassanieni* Bassiouni and Luger (1990), NSF 5.5 m: 17, carapace, dorsal view; 18, left valve, external view. 19, *Cytheropteron* sp., right valve, external view, NSF 15.6 m. 20, *Cytheropteron lugeri* Bassiouni and Morsi (2000), left valve, external view, 05NSC 21 (7.6 m). 21–22 *Cytheropteron ventroliratum* Bassiouni and Morsi (2000), NSF 15.6 m: 21, carapace, dorsal view; 22, right valve, external view. 23–24 *Cytheropteron lekefense* Esker 1968: 23, carapace, dorsal view, NSF 1.5 m; 24, right valve, external view, NSF 0.5 m. 25, species A, right valve, NSF 2.5 m. 26, species B, carapace, left view, NSF 14.4 m. 27, species D, carapace, right view, NSF 6.5 m. 28, *Loxoconcha blanckenhorni* Bassiouni and Luger (1990), carapace, left view, NSF −0.5 m.

sokotoensis, *Monoceratina* sp., *Cytheroptheron lekefense*, *Semicytherura* sp., *Loxoconcha blanckenhorni*, *Megommatocythere denticulata* and species B. *Bythocypris boukharyi* was found only in the 05NSC section (Table 1). These differences can be explained by their rare occurrences in combination with the limited thickness of the 05NSC section.

The ostracod assemblages of the Sidi Nasseur sections show subtle but distinct changes around the main glauconitic level (at height 9.2 m in the NSF section, Fig. 2). *Pontocyprella recurva*, *Pontocypris* sp., *Krithe echolsae*, *Mauritsina coronata*, *Oertliella vesiculosa*, *Ordoniya bulaqensis*, *Reticulina proteros*, *Cytheropteron lekefense* and *Eucytherura* aff. *hassanieni* occur frequently below this level and are rare to absent above. In contrast, *Cytheropteron* sp., *Oertliella delicata*, *Ordoniya ordoniya* and *Protobuntonia nakkadii* are rare to absent below the glauconitic level but occur frequently above it. *Cristaeleberis arabii* shows a distinct peak just above this level (Fig. 5).

These qualitative trends in faunal composition are corroborated by the statistical correspondence analysis. Two sets of census data have been gathered for both the NSF and 05NSC sections: total census data of the ostracods and a second dataset only taking the fraction > 250 μm into account (Table 1). These census data resulted in four different datasets for the statistical analysis: NSF05NSCtot, NSFtot, NSF05NSC250, and NSF250. These names refer to the section and size fraction taken into account. These four datasets were used in the correspondence analysis (Fig. 6) to test if the observed trends appear in both sections and to test if small ostracod species (often not considered in ostracod studies) have any influence on the analysis.

When comparing NSF05NSCtot and NSFtot analyses, the following similarities are observed. CA1 shows the same trend in both datasets (arrow on Fig. 6) although more detail is recorded in the NSF05NSCtot dataset. CA2 of NSFtot is very similar to CA3 of NSF05NSCtot, with again more detail in the latter. NSF05NSC250 and NSF250 show the same trends for CA1, 2 and 3. When comparing the total datasets with the datasets excluding the small ostracods species, similarities are less obvious. Only the dominant trend (observed in CA1) is shared by all datasets (mirrored in 250-datasets).

Based on these observations, it can be concluded that the same trends appear in both sections and that in this case evaluating the >250 μm fraction size is sufficient to observe the dominant trend (CA1) within this fauna. In other words, comparison of this data with other datasets that excluded small ostracod species can be useful.

In the following paragraph, the results for the most complete dataset (NSF05NSCtot) (Fig. 7) will be discussed. R-mode clustering of the ostracod assemblages resulted in two distinct assemblages named after one of their characteristic species. The *R. proteros* assemblage contains all the species that occur frequently below the glauconitic level while the *P. nakkadii* assemblage groups the species that occur frequently above this level (Fig. 7C). Table 2 shows species scores: *R. proteros*, *O. vesiculosa* and *C. lekefense* have a positive score while *C. arabii*, *Xestoleberis tunisiensis*, *Cytheropteron* sp. and *P. nakkadii* have a negative score. The bivariate plot of first two axes of the correspondence analysis gives a similar image with two biofacies: biofacies 1 all samples below the glauconitic level and biofacies 2 groups all samples above this level (Fig. 7B). In fact, this plot clearly demonstrates that only the first axis displays a gradual change across the glauconite marker bed. The scores on the first axes (Fig. 7A) show a decreasing trend with dominantly positive values below and negative values above the glauconitic marker bed. The variability along the second axes is spread across the entire section without a distinct trend.

7.1. Paleoenvironment and paleobiogeography

The paleobiogeography of late early Cretaceous to early Paleocene marine Ostracoda in Arabia and north to equatorial Africa has been recently reviewed and summarized by Luger (2003). Due to the emergence of major parts of the Arabian shield during the Turonian, the uniform 'South Tethyan ostracod province', extending over north–northeast Africa and the Arabian peninsula, was split into a western '*Protobuntonia numidica* ostracod province' (north Africa and western Middle East) and an eastern '*Kaesleria* ostracod province' (eastern Arabia, South Iran and Somalia) by Coniacian times. The separation of these distinct provinces persisted into the early Paleocene.

The ostracod assemblage of the Sidi Nasseur sections belongs to '*Protobuntonia numidica* ostracod province' (Luger, 2003, figs. 8, 9) as reflected in the high numbers of ostracod taxa in common with Egyptian and Israeli sections of equivalent age (Table 3). Some faunal exchange occurred with the 'West-Central African province' as reflected by taxa as *P. nigeriensis*, *P. sokotoensis* and *O. vesiculosa*. Such faunal exchanges occurred already during the Maastrichtian (Luger, 2003).

The ostracod faunas of the Sidi Nasseur section also belong to the South Tethyan Type (STT), as defined by Bassiouni and Luger (1990) in Egypt. The faunal distribution in Egypt is referred to here as there is

Table 1
Total census data of ostracods of the Sidi Nasseur sections

Samples	*Cytherella meijeri*	*Cytherella* cf. *lagenalis*	*Cytherella sinaensis*	*Cytherelloidea ainshamsina*	*Cytherelloidea* aff. *melleguensis*	*Bairdia* sp.	*Bairdia septentrionalis*	*Bairdia malzi*	*Bythocypris aduncа*	*Bythocypris boukharyi*	*Bythocypris eskeri*	*Macrocypris* sp.	*Paracypris eskeri*	*Paracypris jonesi*	*Paracypris nigeriensis*	*Paracypris sokotoensis*	*Paracypris* sp. *B*	*Paracypris* sp.	*Pontocyprella recurva*	*Pontocypris* sp.	*Bythoceratina* sp.	*Monoceratina* sp.	*Krithe echolsae*	*Krithe cf. solomoni*	*Parakrithe crolifa*	*Cytheropteron lekefense*	*Cytheropteron ventroliratum*	*Cytheropteron* sp.
NSF																												
–0.50		1.31	2.18				1.53	1.75	2.84		0.44		3.28	1.53	0.44				0.66			0.22	4.37	1.75	24.67	4.37	2.84	
0.50		1.97	1.48				1.97	0.49					1.97	1.97						1.48			1.48	3.94	14.29	3.94	1.97	
1.50		0.75	1.12		0.75		1.50	1.87	0.75				0.75	0.75		0.75	0.37		1.12	0.75			0.37	0.37	22.80	2.99	14.95	
2.50	0.37	1.10	3.31		0.37		2.67	0.37	1.10				0.74	2.21					1.47	1.10			2.58		12.14	4.42	8.10	
3.20		1.08	2.51				2.69	0.90	0.36			0.24	0.36	1.43					1.79				3.94	2.87	15.77		17.20	
4.50	0.24	1.43	0.95		0.24	0.48	0.95	0.48	5.01				1.19	0.24	0.24				1.19		0.25		0.48	0.72	23.15		7.64	
5.50	1.13	1.80	1.80		1.13		3.38	0.68	2.25				1.58	0.45					0.68				0.45		17.34		10.81	
6.50	0.25	0.75	0.50				1.25	1.25	0.75				1.00					1.25	0.25				0.50	6.02	17.79		4.01	
7.50	0.98	0.98	1.46		1.46		1.71	0.24	0.98				2.44	1.46					0.49				1.71	3.90	18.29	1.95	5.85	
8.50		3.96	0.40		0.79		1.88	1.19					1.58										0.79		20.57		7.91	
8.90	1.15	1.15	1.15		0.86		1.44	0.86	0.29				1.73	0.58	0.29								0.29	2.31	18.73		11.82	2.31
10.00	1.00		1.50				0.63	0.75	1.50				0.50	0.50										1.50	5.50		5.00	3.00
10.50	0.47	1.42	1.18		0.47		1.54	0.36	1.42				1.66	0.95					0.24				1.42	1.42	15.64		17.54	
11.50	0.58	1.16	0.87				4.06	1.60	1.16				2.61	0.58									0.29		24.09		16.84	8.13
12.75	0.67	1.34	0.67		0.22		2.35	0.67	0.22				3.14	0.67		0.22							0.45	0.67	24.86		10.97	3.58
13.60	0.44	0.88	0.88				5.69	0.66					1.97	0.88		0.88								5.47	32.17		6.13	5.25
14.40	0.35	1.40	0.70				1.05	1.66	1.05				2.45	0.35										1.40	18.20		10.50	1.40
15.60	1.45	2.17	1.27	1.45	0.18		2.08	0.27	0.36				1.99	0.72		0.54	0.36						0.74	4.34	35.90		8.86	5.06
16.50		0.74	0.74	1.49			0.74	0.12	0.50				1.98	0.25										4.71	25.77		6.69	2.48
NSC																												
4	3.75	1.30	2.60	2.60									1.30	1.30						1.30				1.30	41.56			
6	4.35	0.88	1.18	1.76		0.59		1.47	0.29	3.53			4.12				0.88		0.88					0.29	38.53		7.06	
10	6.75		0.71	2.86		0.36		0.36	0.71	4.29			1.43	0.36			0.71		0.71	0.71					42.14		2.86	
13	7.6	1.10	0.55	0.83		2.20		0.55		0.55			0.55	2.48										4.96	27.00		6.61	3.31
16	8.4		0.60	1.79		0.30		2.99	0.90	0.30			1.19				0.30		0.30		1.10		2.39	1.49	30.15		7.16	1.19
18	9		0.96	2.40				1.92	0.96		0.48		0.96	2.88					0.96				0.48	1.92	21.63		3.85	
19	9.5		0.40			0.80		1.61		0.40			0.40	2.01										4.42	24.90		6.43	
21	10.3	0.79	1.58	3.56		0.40		2.37	0.79	2.37	0.40		1.98	1.58									0.40	1.58	10.28		2.37	3.95

Samples	*Cytheropteron lugeri*	*Eucytherura aff. hassanteni*	*Semicytherura* sp.	*Loxoconcha blanckenhorni*	*Loxoconcha* sp.	*Mauritsina coronata*	*Mauritsina jordanica nodoreticulata*	*Cristaleberis arabi*	*Megommatocythere denticulata*	*Oertliella vesiculosa*	*Oertliella delicata*	*Oertliella posteriotriangulata*	*Ordonya bulaquensis*	*Ordonya ordonya*	*Paracosta parakefensis*	*Reticulina proteros*	*Protobuntonia nakkadii*	*Xestoleberis tunisiensis*	*Xestoleberis ovata*	Species A.	Species B.	Species C.	Species D.	Total	#ostra/100 g sed	Mass of sample (g)	*N* taxa	Total number of ostracods picked
NSF																											
–0.50				0.87		0.44	1.09	3.71		9.61	1.31	0.66	3.06	3.71	2.40	11.57	0.22	3.71	3.49					100.00	238.1	193.6	30	347
0.50	1.97	19.70				0.49		3.94		5.91		0.99	1.48			4.93		17.73	5.91					100.00	115.9	175.2	22	129
1.50	4.49	4.49	1.50		1.50	1.87	0.37	2.99		2.24		1.12	1.31	1.12	2.24	5.23		4.86	10.47				1.50	100.00	213.5	250.6	33	262
2.50		2.21				4.42		1.84	0.74	16.19	0.74	0.74	4.42	1.84	6.99	4.60		6.99	2.94	1.84		1.47		100.00	405.4	269.1	30	438
3.20		5.73				2.15		1.43		5.02	0.72	1.08	0.72	0.36	6.81	2.15		14.34	8.60					100.00	221.7	250.8	24	280
4.50		5.73				1.19	0.48	0.24		1.43		0.24	4.30	0.24	6.21	0.72		9.55	24.82					100.00	150.8	278.5	29	186
5.50	1.80	14.41				3.60		2.03		3.38	0.23	1.13	0.23	0.68	2.25	3.60		13.29	5.41	0.68		3.60		100.00	266.3	167.1	28	222
6.50	2.01	28.07				1.50	0.25	2.51		2.51	1.00	1.00		0.75	5.01	1.75		11.03	2.01	0.50		2.01	2.26	100.00	232.7	172.3	30	177
7.50	3.90	15.61				1.71		7.07		1.46	0.49	0.24	1.46	2.20	0.98	6.83		7.80	5.85	0.49				100.00	169.0	242.6	29	215
8.50	0.40	3.17				3.96		16.02	0.40	4.75	0.79	0.79	0.40	6.73	3.96	0.79		17.80						100.00	377.1	268.1	22	295
8.90	1.44	14.99				1.15	1.44	5.76		2.31	1.73	1.15		3.46	5.19		0.58	14.99	1.15					100.00	132.6	261.6	27	173
10.00		5.00				2.50	2.13	23.00			3.50	0.50		5.00	13.00		1.50	21.50	1.00					100.00	269.0	297.4	22	386
10.50		4.74				0.47	0.24	5.91			2.61		1.18	2.61	5.45		1.66	17.30	11.85	0.47				100.00	287.7	293.4	26	266
11.50	1.16	6.10			1.45	1.16		3.48		1.74	0.58	0.29	0.87	0.58	1.74	0.58	2.32	11.90	3.48			0.29		100.00	245.5	280.6	29	409
12.75	0.22	1.79				0.45		6.72		1.79	2.24	0.90	1.57	2.24	3.14		0.67	20.16	7.17	0.22				100.00	371.1	241.2	29	299
13.60	2.84				0.88		0.22	2.84			1.09	0.22		0.88	11.60			10.28	6.35		0.66	0.88		100.00	154.2	296.4	24	346
14.40	0.70	3.50			0.70	0.35	1.05	8.78		1.75	0.70	3.15	0.70	5.95	8.05	1.40	2.80	12.25	4.20	0.35	2.80			100.00	368.1	310.5	30	367
15.60	2.17	0.72				0.36	0.41	4.53		0.54	0.72	0.36		2.71	1.45		2.40	9.76	6.15		0.36	0.18		100.00	620.5	356.8	31	376
16.50		3.97				0.25	0.25	1.73		1.49	0.99		0.25	0.25	0.74	0.50	0.74	28.00	11.90		0.99	0.99		100.00	391.6	206.1	28	342
NSC																											
4	3.75		5.19					5.19		2.60	1.30					1.30	1.30	25.97	3.90					100.00	66.90	115.095	16	77
6	4.35	1.18	1.18				0.59	1.47		2.06	0.29	1.18	2.94		7.35			10.88	5.88			3.53		100.00	224.17	149.885	25	169
10	6.75	4.29	7.14			0.36		3.21		1.43					3.93	0.36	0.36	4.64	14.29	0.36		1.43		100.00	194.46	143.988	25	125
13	7.6	4.41	4.41			0.28	0.55	4.96		3.03		1.10	1.65	1.93	1.38	2.75	1.65	11.57	6.61	1.93				100.00	272.96	132.987	28	162
16	8.4		7.16			3.88		10.45		2.69	1.19	0.30	2.09		2.39	1.79		12.54	2.39	0.90		1.19		100.00	222.03	150.883	27	171
18	9		3.85			2.40		5.29		3.37	0.96		1.92	1.92	2.40			8.65	28.85	0.96				100.00	142.82	145.639	23	136
19	9.5					2.01	0.80	8.84		0.80	0.80	0.80	1.61	5.62	10.44	1.20	1.61	20.88					3.21	100.00	160.07	155.56	22	172
21	10.3	0.79			0.79	0.79	0.79	13.04		1.19	2.77	0.40	0.79	5.14	8.30		1.19	23.32	6.32					100.00	965.29	104.839	29	366

(continued on next page)

Table 1 (*continued*)

Samples	*Cytherella meijeri*	*Cytherella* cf. *lagenalis*	*Cytherella sinaensis*	*Cytherelloidea ainshamsina*	*Cytherelloidea* aff. *melleguensis*	*Bairdia* sp.	*Bairdia septentrionalis*	*Bairdia malzi*	*Bythocypris aduncа*	*Bythocypris boukharyi*	*Bythocypris eskeri*	*Macrocypris* sp.	*Paracypris eskeri*	*Paracypris jonesi*	*Paracypris nigeriensis*	*Paracypris sokotoensis*	*Paracypris* sp. *B*	*Paracypris* sp.	*Pontocyprella recurva*	*Pontocypris* sp.	*Bythoceratina* sp.	*Monoceratina* sp.	*Krithe echolsae*	*Krithe* cf. *solomoni*	*Parakrithe crolifa*	*Cytheropteron lekefense*	*Cytheroptheron ventrolitratum*	*Cytheropteron* sp.
NSF																												
–0.50		2.28	3.80				2.66	3.04	4.94		0.76		5.70	2.28	0.76				1.14			0.38	7.60		4.94			
0.50		7.27	5.45				7.27	1.82					7.27	7.27						5.45			5.45		1.82			
1.50		2.34	3.51		2.34		4.68	5.85	2.34				2.34	2.34		2.34	1.17		3.51	2.34			1.17	1.17	8.19			
2.50	0.58	1.75	5.26		0.58		4.23	0.58	1.75				1.17	3.50					2.34	1.75			4.09		1.75			
3.20		3.19	7.45				7.98	2.66	1.06				1.06	4.26					5.32				11.70		1.06			
3.50		11.11					11.11	3.70										22.22							11.11			
4.50	0.92	5.50	5.50		0.92	1.83	3.67	1.83	4.59			0.92	4.59	0.92	0.92				4.59				1.83	2.75	0.92			
5.50	3.38	5.41	5.41		2.70		10.14	2.03	6.76				4.73	1.35					2.03				1.35		3.38			
6.50	0.98	2.94	1.96				4.90	4.90	2.94				3.92					4.90	0.98	0.68	0.98		1.96		6.86			
7.50	2.67	2.67	4.00		4.00		4.67	0.67	2.67				6.67	4.00					1.33				4.00	0.67	9.33			
8.50		10.13	1.01		2.03		4.81	3.04					4.05	1.75									2.03					
8.90		3.51	1.75		2.63		4.39	2.63	0.88				5.26										0.88		8.77		0.88	
9.20	1.61	3.23					22.58	3.23					6.45	3.23											3.23			
10.00	1.08		2.42				1.01	1.21	2.42				0.81	0.81										0.81	1.61			
10.50	1.27	3.23	2.69		1.08		3.49	0.81	3.23				3.76	2.15					0.54				3.23	1.08	19.35		1.08	
11.50	1.37	2.54	1.90				8.89	3.49	2.54				5.71	1.27									0.63		29.84		1.27	
12.75	0.75	2.73	1.37		0.46		4.78	1.37	0.46				6.38	1.37		0.46							0.91	1.37	21.41		0.46	
13.60	0.78	1.50	1.50				9.77	1.13					3.38	1.50		1.50								6.39	27.44		1.50	
14.40	3.14	3.13	1.57				2.35	3.72	2.35				5.48	0.78										1.57	2.35		0.78	
15.60		4.71	2.75	3.14	0.39		4.51	0.59	0.78				4.31	1.57		1.18	0.78							3.14	35.49		0.39	0.39
16.50		2.23	2.23	4.46			2.23	0.37	1.49				6.69	0.74									2.23	5.20	26.77		2.23	1.49
NSC																												
4	3.75	5.88	11.76	11.76									5.88	5.88					2.68	5.88					5.88			
6	4.35	2.68	3.57	5.36		1.79		4.46	0.89	10.71			12.50				2.68		2.74					0.89	2.68			
10	6.75		2.74	10.96		1.37		1.37	2.74	16.44			5.48	1.37			2.74			2.74					13.70			
13	7.6	4.21	2.11	3.16		4.21		2.11		2.11			2.11	9.47					0.95					2.11	2.11			
16	8.4		1.90	5.71		0.95		9.52	2.86	0.95			3.81				0.95		3.13				7.62	4.76	0.95			
18	9		3.13	7.81				6.25	3.13		1.56		3.13	9.38									1.56		7.81			
19	9.5		1.06			2.13		4.26		1.06			1.06	5.32										3.19	7.45			
21	10.3	1.46	2.92	6.57		0.73		4.38	1.46	4.38	0.73		3.65	2.92									0.73		8.76			

Samples	*Cytheropteron lugeri*	*Eucythelura* aff. *hassanteni*	*Semicytherura* sp.	*Loxoconcha blanckenhorni*	*Loxoconcha* sp.	*Mauritsina coronata*	*Mauritsina jordanica nodoreticulata*	*Cristaleberis arabii*	*Megommatocythere denticulata*	*Ornithella vesiculosa*	*Ornithella delicata*	*Ornithella posteroriangulata*	*Ordonya bulaquensis*	*Ordonya ordonya*	*Paracosta parakefensis*	*Reticulina proteros*	*Protobuntonia nakkadii*	*Xestoleberis tunisiensis*	*Xestoleberis ovata*	Species A.	Species B.	Species C.	Species D.	Total	#ostra/100 g sed	Mass of sample (g)	*N* taxa	Total number of ostracods picked
NSF																												
–0.50						0.76	1.90		1.90		16.73	2.28	1.14	5.32	4.56	4.18	20.15	0.38	0.38					100.00	137.4	193.6	13	263
0.50						1.82					21.82		3.64	5.45			18.18							100.00	31.4	175.2	9	55
1.50						5.85	1.17		4.68		7.02		3.51	4.09	3.51	7.02	16.37		1.17					100.00	68.2	250.6	15	171
2.50						7.01			2.92	1.17	25.69	1.17	1.17	7.01	2.92	11.09	7.01		0.58	2.92				100.00	256.0	269.1	13	345
3.20						6.38					12.77	2.13	3.19	2.13		20.21	6.38							100.00	75.0	250.8	10	188
3.50									3.70		22.22		3.70	3.70	1.06	3.70			3.70					100.00	18.0	150.1	5	27
4.50						4.59	1.83		0.92		5.50		0.92	16.51	0.92	23.85	2.75							100.00	39.5	278.5	16	109
5.50						10.81			1.35		10.14	0.68	3.38	0.68	2.03	6.76	10.81		2.03	2.03				100.00	89.2	167.1	13	148
6.50						5.88	0.98		1.96		9.80	3.92	3.92		2.94	19.61	6.86		3.92	0.98			0.98	100.00	60.4	172.3	12	102
7.50						4.67	0.67		3.33		4.00	1.33	0.67	4.00	6.00	2.67	18.67		5.33	1.33				100.00	61.8	242.6	13	150
8.50	1.01					10.13	2.03		14.47	1.01	10.13	2.03	2.03	1.01	14.18	10.13	2.03		1.01					100.00	147.3	268.1	7	195
8.90	0.88					3.51	4.39		14.04		7.02	5.26	3.51		10.53	15.79		1.75						100.00	43.6	261.6	11	114
9.20						6.45			6.45				3.23			25.81	16.13							100.00	13.3	240.3	6	31
10.00						4.03	3.43		32.26			5.65	0.81		8.06	20.97		2.42	9.68					100.00	166.8	297.4	9	248
10.50						1.08	0.54		11.29			6.99		2.69	5.91	12.37		3.76	4.30	3.23	1.08			100.00	126.8	293.4	14	186
11.50		0.63			0.63	2.54			7.62		3.81	1.27	0.63	1.90	1.27	3.81	1.27	5.08	8.89			0.63		100.00	112.3	280.6	11	315
12.75	0.46					0.91			14.05		3.64	4.10	1.82	3.19	4.56	6.38		1.37	8.20	3.64	0.46			100.00	182.8	241.2	14	214
13.60	0.38						0.38		4.891			3.76	0.38			19.92			10.90	1.88		1.13		100.00	89.7	296.4	11	266
14.40						0.78	2.35		0.96		3.91	1.57	7.05	1.57	11.74	18.00	3.13	6.26	7.05		0.78			100.00	164.6	310.5	11	256
15.60						0.78	0.88		6.69		1.18	3.14	0.78		4.31	3.14		5.20	4.31	0.78		0.78	0.39	100.00	285.9	356.8	16	254
16.50						0.74	0.74		5.20		4.46	2.97		0.74	0.74	2.23	1.49	2.23	13.38	6.69				100.00	130.5	206.1	13	269
NSC																												
4	3.75								11.76		11.76	5.88						5.88	5.88	5.88				100.00	14.77	115.095	7	17
6	4.35						1.79		0.89		6.25	0.89	3.57	8.93		22.32				4.46				100.00	74.72	149.885	12	112
10	6.75					1.37			8.22		5.48					15.07	1.37	1.37	1.37		1.37			100.00	50.70	143.988	12	73
13	7.6					1.05	2.11		6.32		11.58		4.21	6.32	7.37	5.26	10.53	6.32	2.11		3.16			100.00	71.44	132.987	10	95
16	8.4					12.38			8.57		8.57	3.81	0.95	6.67		7.62	5.71		1.90		2.86			100.00	69.59	150.883	12	105
18	9					7.81			4.69		10.94	3.13		6.25	6.25	7.81			3.13		3.13			100.00	43.94	145.639	10	64
19	9.5					5.32	2.13		10.64		2.13	2.13	2.13	4.26	6.38	27.66	3.19	4.26	4.26					100.00	60.43	155.56	8	94
21	10.3					1.46	1.46		18.25		2.19	5.11	0.73	1.46	9.49	15.33		2.19	0.73	2.92				100.00	522.71	104.839	12	274

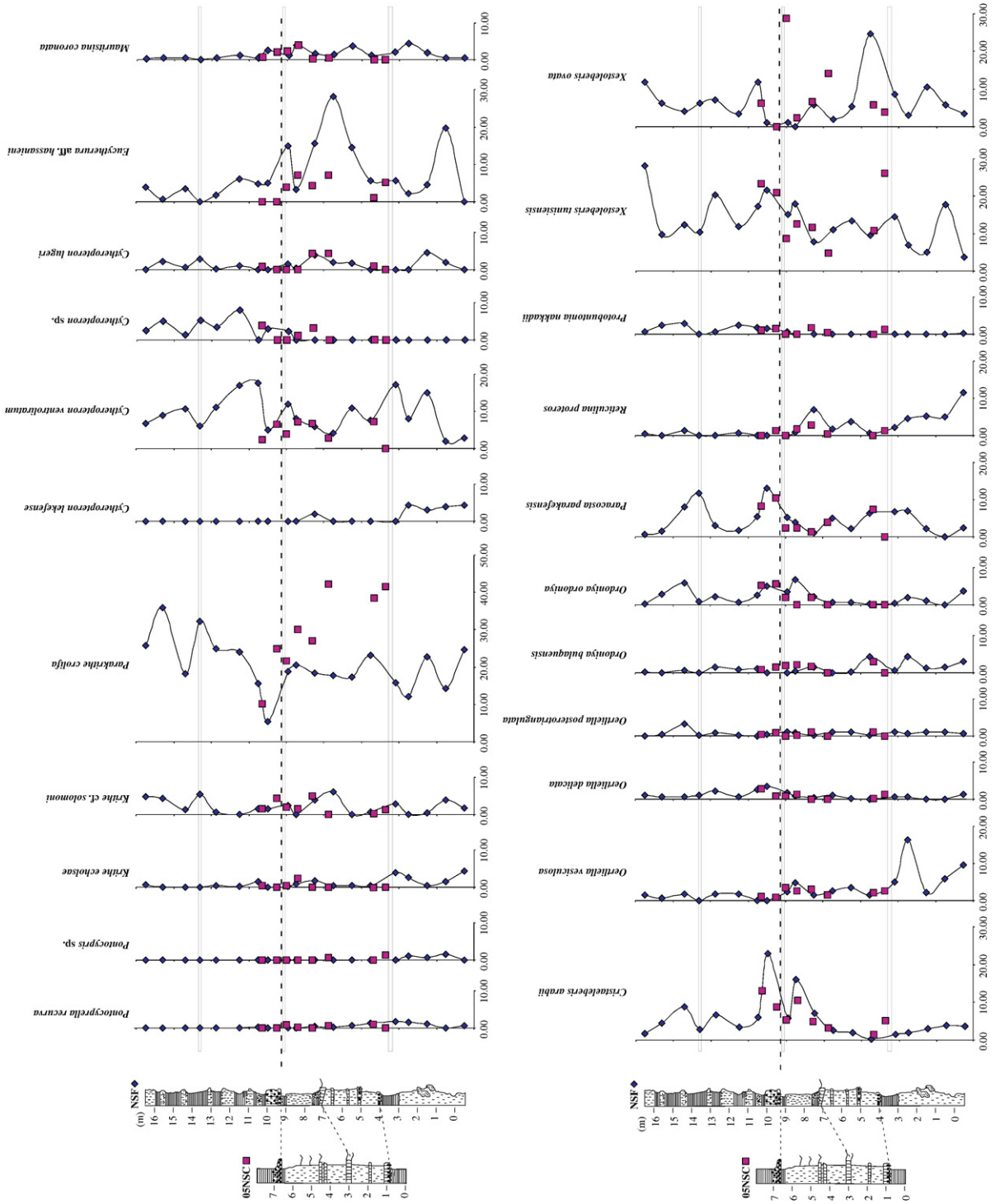

Fig. 5. Relative frequency (%) of important ostracod taxa plotted against depth of the Sidi Nasseur sections, grey areas indicate zones of dissolution.

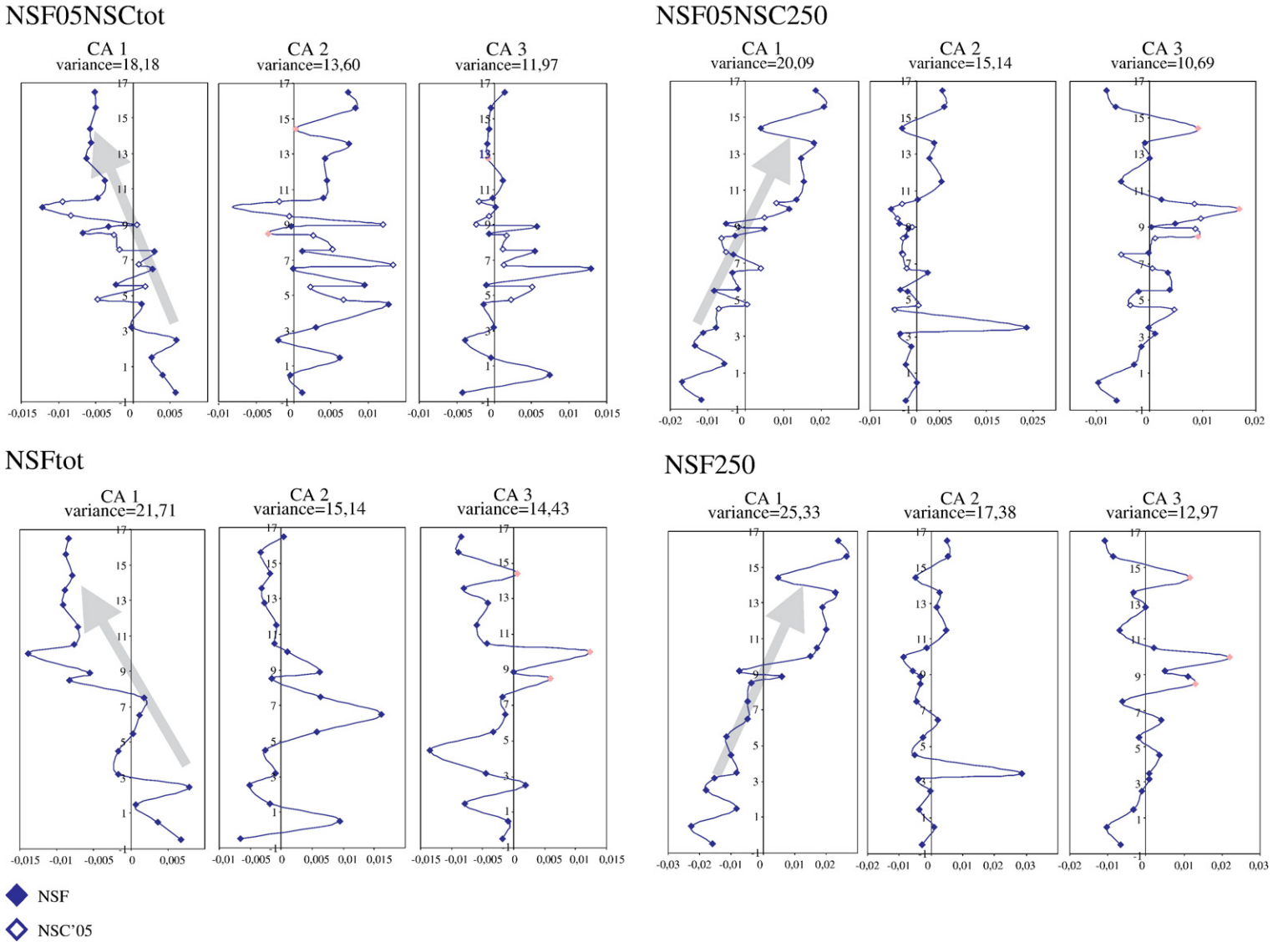

Fig. 6. Comparison of the correspondence analysis of the different ostracods datasets.

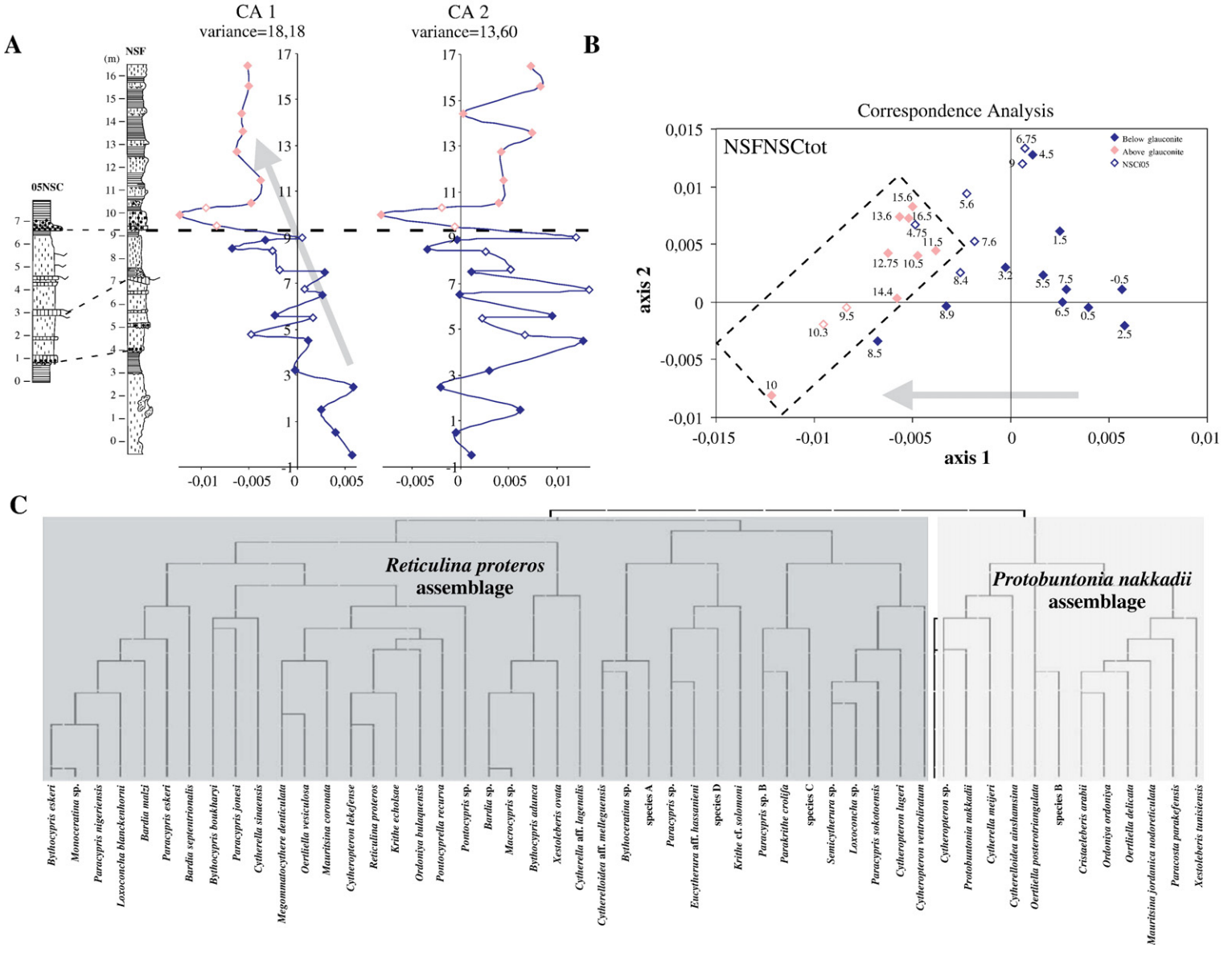

Fig. 7. Correspondence analyses of the NSF05NSCtot dataset. (A) first two axes of correspondence analysis plotted against depth of the Sidi Nasseur sections. (B) bivariate plot of the sample scores on the first two axes resulting from correspondence analysis. (C) R-mode cluster (PAST software, correspondence analysis, hierarchical clustering, pearson correlation, paired-group) of ostracods species.

currently no refined paleobathymetrical distribution model for ostracoda in Tunisia. Typical species for the STT fauna type observed in the studied section are: *Bythocypris adunca*, *C. arabii*, *Cytheroptheron ventroliratum*, *Krithe* cf. *solomoni*, *K. echolsae, M. denticulata*, *O. delicata*, *Oertliella posterotriangulata*, *O. bulaqensis*, *O. ordoniya*, *M. coronata*, *M. jordanica nodoreticulata*, *Paracosta parakefensis*, *Paracypris eskeri*, *P. jonesi*, *Parakrithe crolifa* (morphotype B), *P. recurva*, *R. proteros*, and *X. tunisiensis* (Bassiouni and Luger, 1990). The STT characterizes outer shelf to upper slope environments and is mostly known from other localities in North Africa and the Middle East. A few of the observed species are typically restricted to shallower environments and thus to other fauna types as defined in Egypt): *B. eskeri*, *L. blanckenhorni*, *P. nigeriensis* and *Paracypris sokotoensis* (Table 3). As they are rare in the present assemblages, their occurrences might be explained by displacement and have no implication for the paleodepth estimates. Another species, *O. vesiculosa*, however, does occur in significant numbers in the lower part of the section. In Egypt (Bassiouni and Luger, 1990), this species is typical for the transitional zone between Garra (middle shelf) and Afro-Tethyan (inner shelf) fauna types. As the benthic foraminiferal data indicate outer neritic (>100 m) deposition throughout the Sidi Nasseur sections, *O. vesiculosa* apparently has a wider bathymetric distribution, at least in Tunisia.

Although distinct faunal changes can be observed around the main glauconitic level in the Sidi Nasseur sections, the overall ostracod assemblages range within the STT. If changes in water depth (sea level) are responsible for the changes in the ostracods assemblages, they must have occurred within the outer shelf-upper slope range of the STT. As the benthic foraminiferal data indicate shallowing and more eutrophic conditions across the glauconitic marker bed, it appears that the observed changes in the ostracod assemblage of the Sidi Nasseur sections are related to these parameters.

Previous studies on the ostracod fauna of El Kef (Donze et al., 1982) and Elles (Said, 1978) covered a time-interval from the late Cretaceous to the early Eocene including the D/S transition. Although these studies did not focus on this transition in particular, a comparison of the ostracod assemblages in the three sections around the D/S boundary interval proves instructive. The planktic foraminiferal zones were used to approximately identify the D/S boundary interval. The ostracod assemblages in El Kef and Elles are very similar to those observed in the Sidi Nasseur sections. It is not possible to quantify the similarity due to the large amount of open taxonomy used by Said (1978) and Donze et al. (1982). However, 75% of the species described by Esker (1968) from the Danian of El Kef have been observed at Sidi Nasseur. Danian/Selandian sediments in El Kef and Elles reflect a slightly

Table 2
Species scores of correspondence of the Sidi Nasseur sections

	Component	
	1	2
% of variance	18.18	13.60
Reticulina proteros	0.010875	−0.004418
Oertliella vesiculosa	0.01014	−0.004724
Cytheropteron lekefense	0.010043	−0.004145
Eucytherura aff. *hassanieni*	0.006805	−0.002481
Krithe echolsae	0.005669	−0.002656
Ordoniya bulaquensis	0.004519	0.000386
Pontocyprella recurva	0.003903	0.001255
Pontocypris sp.	0.003257	−0.000319
Xestoleberis ovata	0.003012	0.012101
Species A.	0.002399	−0.000285
Species C.	0.002237	0.001544
Cytheroptheron lugeri	0.002007	0.002075
Semicytherura sp.	0.001945	0.000618
Bythocypris eskeri	0.001938	−0.000969
Mauritsina coronata	0.00193	−0.003064
Cytherella sinaensis	0.001783	0.000136
Bythocypris adunca	0.001754	0.002659
Megommatocythere denticulata	0.001743	−0.001872
Paracypris jonesi	0.001711	−0.000581
Monoceratina sp.	0.001371	−0.000685
Paracypris nigeriensis	0.001252	5.61E−05
Paracypris sp.	0.00111	−0.000842
Loxoconcha blanckenhorni	0.000907	−0.000488
Bairdia malzi	0.000738	−0.000831
Cytherelloidea aff. *melleguensis*	0.000552	−0.000339
Bairdia sp.	0.000519	0.001711
Macrocypris sp.	0.000367	0.00121
Paracypris sp. *B*	0.000358	0.002056
Bythoceratina sp.	0.000174	0.00021
Oertliella posterotriangulata	6.05E− 05	−0.001676
Cytherella cf. *lagenalis*	−2.91E− 05	−0.000354
Paracypris eskeri	−3.51E− 05	0.000573
Bairdia septentrionalis	−5.25E− 05	−0.000203
Species D.	−7.11E− 05	−0.001812
Bythocypris boukharyi	−0.000579	0.000618
Paracypris sokotoensis	−0.000604	0.001219
Parakrithe crolifa	−0.000614	0.007533
Loxoconcha sp.	−0.000665	0.000191
Krithe cf. *solomoni*	−0.000977	−0.000242
Cytheroptheron ventroliratum	−0.001097	0.000599
Cytherella meijeri	−0.001648	−4.50E− 05
Cytherelloidea ainshamsina	−0.001884	0.001989
Mauritsina jordanica nodoreticulata	−0.002366	−0.002119
Species B.	−0.002826	4.14E− 05
Oertliella delicata	−0.003589	−0.002348
Ordoniya ordoniya	−0.004657	−0.005528
Protobuntonia nakkadii	−0.00474	−0.000507
Paracosta parakefensis	−0.005239	−0.002801
Cytheropteron sp.	−0.007241	0.00078
Xestoleberis tunisiensis	−0.007636	−0.002423
Cristaeleberis arabii	−0.008731	−0.0078

Table 3
Stratigraphic/geographic distribution and paleoenvironmental interpretation of studied ostracod taxa (data from Esker, 1968; Bassiouni, 1969; Bassiouni, 1970; Donze et al., 1982; Honigstein, 1984; Bassiouni and Luger, 1990; Honigstein and Rosenfeld, 1995; Morsi, 1999 Bassiouni and Morsi, 2000)

	Cretaceous	Paleocene						Eocene	Paleoecological interpretation		
	Maastrichtian	Danian			Selandian	Thanetian					
		Pa	P1	P2	P3	P4	P5	P6			
Cytherelloidea melleguensis Damotte and Said, 1982	T								Shallow, warm water (outer infraneretic)		
Eucytherura hassanieni Bassiouni and Luger, 1990	E										
Macrocypris sp. Donze et al., 1982	T	T	T	T							
Paracypris eskeri Bassiouni and Morsi, 2000	T	T	T	T/E	E				Middle to outer shelf		
Protobuntonia nakkadii Bassiouni, 1970	T/E	T/J	T/J	T/J	T/E/J	T			Middle shelf		
Krithe echolsae Esker, 1968	T/I	T/E/I	T/E/I	T/E/I	T/E/I	E/I	E/I		Outer shelf		
Oertliella vesiculosa (Apostolescu, 1961)	T	Su/T	Su/T	Su/T	T	M/L	M/L/E		Shallow euhaline shelf		
Paracypris nigeriensis Reyment, 1960	N	N /L/I	N /L/I	N /L/I	N /I	N /I	N /I	E/I	Inner euhaline shelf	Nigeria	N
Mauritsina coronata (Esker, 1968)	T	T/J/E/I	T/J/E/I	T/J/E/I	T/J/E/I	T/J/E/I	J/E/I	J/E/I	Outer shelf	Egypt	E
Mauritsina jordanica nodoreticula Bassiouni, 1970	T	T/E/I	T/E/I	T/E/I	J/T/E/I	E/I	E/I	E/I	Outer shelf	Tunisia	T
Megommatocythere denticulata (Esker, 1968)	T	T/E	T/E	T/E	E	E	E	E	Outer shelf	Israel	I
Ordoniya ordoniya (Bassiouni, 1970)	T	T/J/E	T/J/E	T/J/E	J/E	E	E	E	Outer shelf	Jordan	J
Pontocyprella recurva Esker, 1968	T	T/E	T/E	T/E	E	E	E	E	Outer shelf	Mali	M
Xestoleberis tunisiensis (Esker, 1968)	T	T	T	T/E	E	E	E	E	Outer to inner shelf	Libya	L
Bythocypris adunca Esker, 1968	T	T	T	T		E	E	E	Outer shelf	Sudan	Su
Bairdia septentrionalis Bonnema, 1941		T	T	T						Senegal	Se
Bairdia aff. *septentionalis* Bonnema, 1941		E/I	E/I	E/I	E/I	E/I	E/I				
Cristaeleberis arabii Bassiouni, 1970		J	J	J/E	J/E				Middle to outer shelf		
Cytherella cf. *lagenalis* Marlière, 1958 in Morsi, 1999		E	E	E	E	E	E		All water depths		
Cytherella sinaensis Morsi, 1999		E	E	E	E	E	E		All water depths		
Bythocypris boukharyi Bassiouni and Morsi, 2000		N/Se	N/Se	N/Se	N/Se	E/N/Se	E/N/Se	E			
Oertliella posterotriangulata Morsi, 1999		E/I	E/I	E/I	E/I	E/I	E/I	E/I	Outer shelf		
Ordoniya bulaquensis Bassiouni and Luger, 1990		T/E/I	T/E/I	T/E/I	T/E/I	E/I	E/I	E/I	Outer shelf		
Paracosta parakefensis Bassiouni and Luger, 1990		E	E	E	E	E	E	E	Mainly outer, rarely middle shelf		
Paracypris jonesi Bonnema, 1940		T	T	T/E	E	E	E	E	Inner to outer shelf		
Parakrithe crolifa Bassiouni and Luger, 1990		E/I	E/I	E/I	E/I	E/N/I	E/N/I	E/I	A inner euhaline shelf, B outer shelf		
Reticulina proteros Bassiouni, 1969		T/J/I	T/J/I	T/J/I	T/J/I	T/J/E/I	T/J/E/I	T/J/E/I	Middle to outer shelf		
Paracypris sp. B Esker, 1968		T	T	T				E			
Bythocypris eskeri Bassiouni and Luger, 1990		T	T	T		N	N/E	E	Euhaline inner shelf deposits		
Cytherella meijeri Esker, 1968		T	T	T		E	E	E	All water depths		
Cytheropteron lekefense Esker, 1968		T	T	T		E	E	E			
Oertliella delicata Bassiouni and Luger, 1990				E	E	E	E		Middle to outer shelf		
Cytheropteron ventroliratum Bassiouni and Morsi, 2000				E	E	E	E	E			
Krithe cf. *solomoni* Honigstein, 1984					E	E			Outer shelf		
Paracypris sokotoensis Reyment, 1981						Se/N/E	Se/N/E	Se/E	Rare in euhaline inner shelf, middle to outer shelf		
Cytheropteron lugeri Bassiouni and Morsi, 2000						E	E	E			
Loxoconcha blanckenhorni Bassiouni and Luger, 1990						E	E	E	Middle shelf		
Bairdia malzi Morsi and Speijer, 2003						E	E	E	Outer shelf		
Cytherelloidea ainshamsina Bassiouni and Morsi, 2000								E	Shallow, warm waters (outer infraneretic)		

deeper paleodepth than Sidi Nasseur, ~ 200 m in the Danian and ~ 150 m in the Selandian (Guasti et al., 2006). Yet the ostracod assemblages of all three sections belong to the STT ostracod fauna as defined by Bassiouni and Luger (1990). The depth range of the STT ostracod fauna appears to be too broad to estimate the paleobatymetrical differences between different Tunisian sections, independently. A refinement of outer shelf ostracod faunatypes as defined by Bassiouni and Luger (1990) based on quantitative instead of qualitative or semi-quantitative data could allow for more detailed paleoenvironmental reconstructions on the basis of ostracods.

The transition in ostracod assemblages at the glauconitic marker bed is also characterized by a change in paleoproductivity as the environment evolves from an oligotrophic to eutrophic setting at the P3a–P3b subzonal transition (see also Guasti et al., 2006).

Donze et al. (1982, fig. 4) observed the replacement of *Krithe* and *Parakrithe* morphotype 2 by morphotype 3 in the El Kef section around the P3a–P3b subzonal transition. Our data show a similar evolution: with a mix of *K. echolsae* (belonging to morphotype 2) and *Krithe* cf. *solomoni* (belonging to morphotype 3) occurring below the P3a–P3b subzonal transition, while only *Krithe* cf. *solomoni* occurs frequently above it (Fig. 5). Based on the hypothesis of Peypouquet (1979) that size and shape of the anterior vestibulum of *Krithe* and *Parakrithe* are related to oxygen levels, Donze et al. (1982) constructed a curve of the estimated levels of dissolved oxygen of the El Kef section. This curve shows fluctuations around the P3a–P3b subzonal transition and a general trend of decreasing O_2-levels during Subzone P3b. However, studies on the recent distribution of *Krithe* and *Parakrithe* have provided strong proof against the Peypouquet-hypothesis (Whatley and Quanhong, 1993; van Harten, 1996) and therefore we refrain from interpreting the trends in the *Krithe*-species in terms of oxygen levels. Although the driving biological factor is unknown, it remains noteworthy that both the El Kef and Sidi Nasseur sections display the same trend. Another hypothesis, proposed by van Harten (1995), explains the variability in the vestibula of *Krithe* by differential sense perception and food-detection. According to this hypothesis, the evolution in Krithe in El Kef and Sidi Nasseur are related to food availability. This corresponds well with the observed changes in paleoproductivity at the same level (Guasti et al., 2006).

8. Tunisian Danian/Selandian boundary sections (synthesis and comparison with other regions)

8.1. Stratigraphy

The D/S boundary interval in the Sidi Nasseur section is characterized by at least two unconformities. The first co-occurs with the P2/P3a subzonal boundary, coinciding with the D/S boundary as recognized by Berggren et al. (1995, fig. 1). The second unconformity occurs at the base of the main glauconitic bed and coincides with the P3a/P3b subzonal boundary. As demonstrated above, the main biotic changes, both in ostracods and foraminifera, occur at this level. We believe that the second unconformity most likely correlates with the D/S boundary in the type region. Recent work in Denmark has demonstrated that the D/S boundary is situated near the NP4/NP5 zonal boundary (Clemmensen and Thomsen, 2005). This corresponds to a level close to the P3a/P3b subzonal boundary in the scheme of Berggren et al. (1995). The position of the P2/P3 zonal boundary in the North Sea Basin is uncertain. However, Schmitz et al. (1998) place the D/S boundary in the Zumaya section, a potential GSSP candidate, also near the NP4/NP5 zonal boundary and well above the P2/P3a subzonal boundary. Similar to the Danish basin, this level at Zumaya and in other sections in northern Spain corresponds to a remarkable change from limestone to marl deposition (Schmitz et al., 1998; Baceta et al., 2006), a feature that may relate to an important phase in the tectonic evolution of the north Atlantic and NW Europe (Nielsen et al., 2005). Also in Egypt, the main faunal changes in the D/S transition occur just below to the P3a/b subzonal boundary (Speijer, 2003; Guasti et al., 2005b) and appear correlative to those in Tunisia (Guasti, 2005). Furthermore, the presence of a thick glauconite bed in the Sidi Nasseur section in a similar stratigraphic position as the Selandian Lellinge greensands in Denmark (e.g. Clemmensen and Thomsen, 2005) may be significant with respect to changing depositional settings in the D/S transition. Based on the arguments above, we conclude that in the Sidi Nasseur section the D/S boundary is best placed at the P3a/P3b subzonal boundary. Studies on other Tunisian sections have shown similar faunal changes at the P3a/P3b subzonal boundary (Donze et al., 1982; Guasti et al., 2005a; 2006) suggesting the same characterization of the D/S boundary. The glauconite bed observed also at Elles (Guasti et al., 2006) and in the Garn Halfaya section, between El Kef and Sidi Nasseur (unpubl. data J. Sprong) indicates that the D/S boundary in northern Tunisia is characterized by a regional hiatus due to erosion of the top of Subzone P3a. If correct, this would rule out any section in the Tunisian Trough as a potential GSSP for the D/S boundary.

8.2. Sea-level and climate

Based on the sedimentologic and faunal changes, the D/S transition in the Sidi Nasseur section is characterized by an important sequence boundary (SB). In Egypt, this interval is also characterized by a SB although it is expressed quite differently in the sediments and biota. The D/S transition in Egypt is characterized by a dark brown organic-rich marl bed, similar to a black shale (laminated, full of fish remains and planktic foraminifera; Speijer, 2003; Guasti et al., 2005b). Although, a similar sea-level evolution was observed at the D/S

transition in Tunisia, there is no indication of a D/S black shale bed at Sidi Nasseur. Depositional conditions in the early Selandian were different between the Tunisian Trough and the Nile Valley Basin and erosion may have removed the beds correlative to the black shale.

Also in the Zumaya section (Schmitz et al., 1998) and in the North Sea Basin (Clemmensen and Thomsen, 2005), the D/S transition is characterized by an important SB. Some evidence indicates that sea-level changes in this time-interval are of tectonic nature (Nielsen et al., 2005). However, as shown by the comparison of D/S transitions in different basins, it appears that the sea-level changes at the D/S boundary also comprise a eustatic signature and that the Sel1-sequence (as defined by Hardenbol et al., 1998 in the North Sea Basin) can be traced into Africa. As the Paleocene is generally considered as an ice-free, greenhouse world (Zachos et al., 2001), the mechanism behind these eustatic sea-level fluctuations is uncertain and thus the eustatic nature of these events remains equivocal. Speijer (2003) speculated on the existence of ice sheets in the Paleocene to explain the eustatic sea-level change observed at the D/S boundary in Egypt and more recently, Miller et al. (2005) have argued that only glacioeustacy can account for rapid eustatic sea-level change with amplitudes >20 m in the late Cretaceous to early Paleogene greenhouse.

9. Conclusions

The D/S boundary at Sidi Nasseur corresponds to a sequence boundary as indicated by truncated ranges of stratigraphic markers and at a glauconitic marker bed. This bed coincides with changes in benthic foraminiferal and ostracod assemblages. The *R. proteros* assemblage, with the typical species *R. proteros*, *O. vesiculosa* and *C. lekefense*, is gradually replaced by the *P. nakkadii* assemblage, with the typical species *C. arabii*, *X. tunisiensis*, *Cytheropteron* sp. and *P. nakkadii*, at the D/S boundary. These changes are related to an overall drop in sea level and a rise in paleoproductivity. Similar faunal and lithological changes have been observed in other Tunisian sections. The D/S boundary in its type area and in the proposed GSSP section of Zumaya is situated within Subzone P3a. As a large part of this zone is missing at Sidi Nasseur, the D/S boundary coincides with the P3a/P3b subzonal boundary rendering this section an unsuitable GSSP candidate. Yet in combination with other sections in the basin, the Sidi Nasseur section provides an important window on paleoenvironmental evolution during the earliest Paleogene.

Acknowledgements

Sander Ernst and Ivo Duijnstee are thanked for help with statistical issues. Karel Wouters kindly provided essential literature for this study. The SEM-pictures were made with the professional help of Julien Cilis, for which we owe him our thanks. A.M.M. Morsi kindly provided us with taxonomic suggestions concerning more enigmatic ostracod specimens. This project was financially supported by the Research Foundation – Flanders (FWO Vlaanderen) and the Research fund of the KULeuven.

Appendix A. Supplementary data

Supplementary data associated with this article can be found, in the online version, at doi:10.1016/j.marmicro.2006.08.006.

References

Aubert, J., Berggren, W.A., 1976. Paleocene benthic foraminiferal biostratigraphy and paleoecology of Tunisia. Bulletin des Centres de Recherches, Pau-SNPA 10, 379–469.

Baceta, J.I., Bernaola, G., Arostegi, J., 2006. Lithostratigraphy of the Mid-Paleocene interval at Zumaia section. In: Bernaola, G., Baceta, J.I., Payros, A., Orue-Etxebarria, X., Apellaniz, E. (Eds.), The Paleocene and lower Eocene of the Zumaia section (Basque Basin). Climate and Biota of the Early Paleogene 2006. Post conference Field Trip Guidebook, Bilbao. 82 pp.

Bassiouni, M.E.A.A., 1969. Einige Costa-und Carinocythereis(Reticulina)-Arten aus dem Paläozän und Eozän van Jordanien (Ostracoda). Neues Jahrbuch fur Geologie und Paläontologie, Abhandlungen 134, 1–16.

Bassiouni, M.E.A.A., 1970. Ostracoda (Mauritsininae und Trachyleberidinae) und ihre Bedeutung für die Biostratigraphie des Maastricht und des Alttertiär von Jordanien. Beihefte zum Geologischen Jahrbuch 106, 5–52.

Bassiouni, M.E.A.A., Luger, P., 1990. Maastrichtian to early Eocene ostracoda from southern Egypt. Palaeontology, palaeoecology, palaeobiogeography and biostratigraphy. Berliner geowissenschaftliche Abhandlungen, Reihe A 120, 755–928.

Bassiouni, M.E.A.A., Morsi, A.-M.M., 2000. Paleocene–Lower Eocene ostracodes from El Quss Abu Said Plateau (Farafra Oasis), Western Desert, Egypt. Palaeontographica. A 257, 27–84.

Berggren, W.A., Kent, D.V., Swisher, C.C.I., Aubry, M.-P., 1995. A revised Cenozoic geochronology and chronostratigraphy. In: Hardenbol, J. (Ed.), Geochronology, time scales and global stratigraphic correlation. Society of Economic Paleontologists and Mineralogists, Special Publication, vol. 54, pp. 129–212.

Berggren, W.A., Aubry, M.-P., van Fossen, M., Kent, D.V., Norris, R.D., Quillevere, F., 2000. Integrated Paleocene calcareous plankton magnetobiochronology and stable isotope stratigraphy: DSDP Site 384 (NW Atlantic Ocean). Palaeogeography, Palaeoclimatology, Palaeoecology 159, 1–51.

Burollet, P.F., 1956. Contribution à l'étude stratigraphique de la Tunésie centrale. Annales des Mines et de la Géologie 18, 1–350.

Clemmensen, A., Thomsen, E., 2005. Palaeoenvironmental changes across the Danian–Selandian boundary in the North Sea Basin. Palaeogeography, Palaeoclimatology, Palaeoecology 219, 351–394.

Cowie, J.W., Ziegler, W., Remane, J., 1989. Stratigraphic commission accelerates progress, 1984–1989. Episodes 12, 79–83.

Desor, E., 1847. Sur le terrain danien, nouvel étage de la craie. Bulletin de la Société Géologique de France 4, 179–182.

Donze, P., Colin, J.-P., Damotte, R., Oertli, H.J., Peypouquet, J.-P., Said, R., 1982. Les ostracodes du Campanien terminal à l'Eocène inférieur de la coupe du Kef, Tunésie nord-occidentale. Bulletin des Centres de Recherches Exploration-Production Elf Aquitaine 6, 273–335.

Dupuis, C., Steurbaut, E., Molina, E., Rauscher, R., Tribovillard, N., Arenillas, I., Arz, J.A., Robaszynski, F., Caron, M., Robin, E., Rocchia, R., Lefevre, I., 2001. The Cretaceous–Paleogene (K/P) boundary in the Aïn Settara section (Kalaat Senan, Central Tunesia): lithological, micropaleontological and geochemical evidence. Bulletin de l'Institut Royale des Sciences Naturelles de la Belgique– Sciences de la Terre 71, 169–190.

Esker, G.C.I., 1968. Danian ostracods from Tunisia. Micropaleontology 14, 319–333.

Gradstein, F.M., Ogg, J.G., Smith, A.G. (Eds.), 2004. A Geological time scale 2004. Cambridge University Press, Cambridge. 610 pp.

Guasti, E., 2005. Early Paleogene environmental turnover in the Southern Tethys as recorded by foraminiferal and organic-walled dinoflagellate cysts assemblages. Berichte aus dem Fachbereich Geowissenschaften der Universität Bremen 241, 1–203.

Guasti, E., Kouwenhoven, T.J., Brinkhuis, H., Speijer, R.P., 2005a. Paleocene sea-level and productivity changes at the southern Tethyan margin (El Kef, Tunisia). Marine Micropaleontology 55, 1–17.

Guasti, E., Speijer, R., Fornaciari, E., Schmitz, B., Kroon, D., Gharaibeh, A., 2005b. Paleoenvironmental change at the Danian–Selandian transition in Tunisia: planktic formainifera and organic-walled dinoflagellate cysts records. Early Paleogene environmental turnover in the Southern Tethys as recorded by foraminiferal and organic-walled dinoflagellate cysts assemblages. Berichte aus dem Fachbereich Geowissenschaften der Universität Bremen, vol. 241, pp. 75–110.

Guasti, E., Speijer, R., Brinkhuis, H., Smit, J., Steurbaut, E., 2006. Paleoenvironmental change at the Danian–Selandian transition in Tunisia: planktic formainifera and organic-walled dinoflagellate cysts records. Marine Micropaleontology 59, 210–229.

Hammer, Ø., Harper, D.A.T., Ryan, P.D., 2001. PAST: Paleontological Statistics software package for education and data analysis. Palaeontologia Electronica 4 (9 pp.).

Hardenbol, J., Thierry, J., Farley, M.B., De Graciansky, P.-C., Vail, P.R., 1998. Mesozoic and Cenozic sequence chronostratigraphic framework of European basins. In: Vail, P. (Ed.), Mesozoic and Cenozoic Sequence Stratigraphy of European Basins. SEPM Special Publication, vol. 60, pp. 3–13.

Honigstein, A., 1984. Senonian ostracodes from Israel. Geological Survey of Israel, Bulletin 78, 1–48.

Honigstein, A., Rosenfeld, A., 1995. Palaeocene ostracods from southern Israel. Revue de Micropaleontologie 38, 49–62.

Jorissen, F.J., de Stigter, H.C., Widmark, J.G.V., 1995. A conceptual model explaining benthic foraminiferal microhabitats. Marine Micropaleontology 26, 3–15.

Kouwenhoven, T.J., Speijer, R.P., Van Oosterhout, C.W.M., Van Der Zwaan, G.J., 1997. Benthic foraminiferal assemblages between two major extinction events: the Paleocene El Kef section, Tunisia. Marine Micropaleontology 29, 105–112.

Luger, P., 2003. Paleobiogeography of late Early Cretaceous to Early Paleocene marine Ostracoda in Arabia and North to Equatorial Africa. Palaeogeography, Palaeoclimatology, Palaeoecology 196, 319–342.

Martini, E., 1971. Standard Tertiary and Quaternary calcareous nannoplankton zonation. In: Farinacci, A. (Ed.), Proceedings of the 2nd Planktonic Conference, Rome, 1970. Tecnoscienza, Rome, pp. 739–785.

Miller, K.G., Wright, J.D., Browning, J.V., 2005. Visions of ice sheets in a greenhouse world. Marine Geology 217, 215–231.

Morsi, A.-M.M., 1999. Paleocene to Early Eocene ostracodes from the area of east-central Sinai, Egypt. Revue de Paléobiologie 18, 31–55.

Nielsen, S.B., Thomsen, E., Hansen, D.L., Clausen, O.R., 2005. Plate-wide stress relaxation explains European Palaeocene basin inversions. Nature 435, 195–198.

Peypouquet, J.-P., 1979. Ostracodes et paléoenvironnements. Methodologie et application aux domaines profonds du Cénozoique. Bulletin du Bureau de Recherches Géologiques et Minières 4, 3–79.

Remane, J., Keller, G., Hardenbol, J., Ben Haj Ali, M., 1999. International workshop on Cretaceous–Paleogene transitions in Tunisia: the El Kef stratotype for the Cretaceous–Paleogene boundary reconfirmed. Episodes 22, 47–48.

Rosenkrantz, A., 1924. De københavnske Grønsandslag og deres Placering i den danske Lagrække. Meddelelser fra Dansk Geologisk Forening 6, 1–39.

Said, R., 1978. Etude stratigraphique et micropaléontologique du passage Crétacé–Tertiaire du synclinal d'Elles (Région Siliana-Sers), Tunésie centrale. PhD Thesis, Université de Paris VI, Paris, 275 pp.

Saint-Marc, P., Berggren, W.A., 1988. A quantitative analysis of Paleocene benthic foraminiferal assemblages in central Tunisia. Journal of Foraminiferal Research 18, 97–113.

Salaj, J., 1980. Microbiostratigraphie du Crétacé et du Paléogène de la Tunésie septentrionale et orientale (hypostratotypes tunisiens). Institut Géologique de Dionyz Stur, Bratislava (238 pp.).

Schimper, W.P., 1874. Traité de Paléontologie végétale 3 Paris.

Schmitz, B., Molina, E., von Salis, K., 1998. The Zumaya section in Spain: a possible global stratotype section for the Selandian and Thanetian Stages. Newsletter on Stratigraphy 36, 35–42.

Speijer, R., 2003. Danian–Selandian sea-level change and biotic excursion on the southern Tethyan margin. In: Thomas, E. (Ed.), Causes and consequences of globally warm climates in the Early Paleogene. Geological Society of America, Special Paper, vol. 369, pp. 275–290.

Speijer, R.P., Schmitz, B., 1998. A benthic foraminiferal record of Paleocene sea level and trophic/redox conditions at Gebel Aweina, Egypt. Palaeogeography, Palaeoclimatology, Palaeoecology 137, 79–101.

Steurbaut, E., Dupuis, C., Arenillas, I., Molina, E., Matmati, M.F., 2000. The Kalaat Senan section in central Tunisia: a potential reference section for the Danian/Selandian boundary. GFF 122, 158–160.

van Harten, D., 1995. Differential food detection: a speculative reinterpretation of vestibule variability in Krithe (Crustacea: Ostracoda). In: Riha, J. (Ed.), Ostracoda and Biostratigraphy. Balkema, Rotterdam, pp. 33–36.

van Harten, D., 1996. The case against *Krithe* as a tool to estimate the depth and oxygenation of ancient oceans. In: Moguilevsky, A., Whatley, R. (Eds.), Microfossils and oceanic environments. University of Wales, Aberystwyth-Press, pp. 297–304.

Varol, O., 1989. Paleocene calcareous nannofossil biostratigraphy. In: van Heck, S.E. (Ed.), Nannofossils and their applications. Ellis Horwood Ltd., Chichester, pp. 267–310.

Whatley, R., Quanhong, Z., 1993. The Krithe problem: a case history of the distribution of *Krithe* and *Parakrithe* (Crustacea, Ostracoda) in the South China Sea. Palaeogeography, Palaeoclimatology, Palaeoecology 103 (3–4), 281–297.

Zachos, J., Pagani, M., Sloan, L., Thomas, E., Billups, K., 2001. Trends, rhythms, and aberrations in global climate 65 Ma to present. Science 292, 686–693.

Zaier, A., Beji-Sassi, A., Sassi, S., Moody, R.T.J., 1998. Basin evolution and deposition during the Early Paleogene in Tunisia. In: Clark-Lowes, D.D. (Ed.), Petroleum Geology of North Africa. Special Publication, vol. 132. Geological Society, London, pp. 375–393.